Journal of Marine Research, 58, 61–95, 2000

Floats and *f/H*

by J. H. LaCasce[1]

ABSTRACT

The sensitivity of oceanic float dispersion to *f/H*, where *H* is a spatially filtered representation of the water depth, is examined with floats from the Atlantic and Pacific oceans. The first and second moments of the displacements relative to *f/H* were found and compared to those for zonal and meridional displacements. In all cases, the moments relative to *f/H* display equal or greater anisotropy than those relative to geographical coordinates, suggesting a preferred tendency for spreading along *f/H*. In regions where the topography is flat (at the equator, in the interior South Atlantic and in the North Pacific), transport is much greater along than across latitude lines, and the moments relative to *f/H* are essentially the same. But the results differ where the topography is steep (the North Atlantic and near the western boundary in the Equatorial and South Atlantic), where anisotropic spreading relative to *f/H* occurs even though the geographical moments are isotropic or meridionally-enhanced. Only in the North Pacific, where the topography is smaller scale and less steep, is the spreading more anisotropic in geographical coordinates. The present method is tested using trajectories from a stochastic model, and correctly shows that no such tendency for spreading along *f/H* exists. Mean and eddy effects are discussed, but are not believed to be well resolved.

1. Introduction

The statistical analysis of oceanic float data was greatly influenced by the pioneering work of Freeland *et al.* (1975), who used various analyses to deduce dynamical characteristics in the western North Atlantic. Among other things, they calculated zonal and meridional diffusivities (measures of lateral mixing in those directions). In subsequent papers, R. Davis formalized a procedure of calculating mean flows and diffusivities from float data, allowing in particular for laterally-varying means and diffusivities (see Davis, 1991). His method also concerns statistical quantities in the zonal and meridional directions.

However, with topography tracer transport need not be oriented zonally or meridionally. For instance, the strongest currents over the continental shelf are generally those parallel to the isobaths, and shelf studies are often set in a frame rotated accordingly. Because topography varies greatly, such a simple rotation is not realistic on the gyre scale, but it is possible nevertheless to account for variable topography in defining particle dispersion.

1. Woods Hole Oceanographic Institution, Woods Hole, Massachusetts, 02543, U.S.A. ***email: jlacasce@whoi.edu***

There are a number of ways one might do this. The present approach, introduced in an earlier work (LaCasce and Speer, 1999; LS hereafter), involves rotating axes at each point along a particle trajectory. Given a continuous two-dimensional field, say water depth, one can define a gradient vector at every point in the domain; then instantaneous particle velocities can be projected onto axes parallel and perpendicular to the field contours (e.g. the isobaths) at each point. Integrating the resulting velocities in time yields net displacements along and across contours.

If motion across the contours of a given field is inhibited for some reason, the displacement along those contours will generally be greater. An obvious example concerns potential vorticity (PV), because fluid parcels conserve PV in the absence of forcing and so cannot drift ceaselessly across the (mean) PV contours. LS considered various idealized barotropic flows and used projected displacements to demonstrate how particle drift was aligned with f/H. In particular, they showed how the first and second moments of the displacements (the mean and dispersion) were more anisotropic with respect to f/H than to (x, y). Interestingly, one obtains an additional bit of information with this approach: the rate at which those moments change. This in turn can provide hints about the underlying Eulerian flow; in several of the cases considered where the dispersion in (x, y) suggested "anomalous" diffusion (e.g. Solomon *et al.,* 1993), the f/H dispersion indicated a simple shear flow (LS).

In the present work, we will examine oceanic float statistics relative to f/H. There are two reasons for doing so. One is simply to illustrate how the method can be applied with actual data and a given stationary (and possibly noisy) field. Indeed, f/H is one among many possibilities. Second is to examine whether f/H has relevance for Lagrangian motion in the subsurface ocean (because the ocean is stratified and driven by both the wind and thermohaline processes, it's not obvious that it ought to be).

A sample calculation presented in LS suggested that floats below 1000 m in the North Atlantic are sensitive to barotropic f/H. In the present work many more floats are examined to discover whether such a sensitivity varies with region and/or with depth. Float trajectories from the North Atlantic, the Equator, the South Atlantic and the North Pacific are used, and a range of depths considered. Following LS, the focus will be on the first and second moments of the displacements, i.e. the mean and the dispersion.

Previous authors have noted how floats are often influenced by f/H (e.g. Rossby *et al.,* 1983). Others have described how topography can affect float statistics (e.g. Freeland *et al.,* 1975) and how it can even influence surface drifter motion (Richardson, 1982). As will be seen, the present results suggest a degree of steering by f/H in many regions, and at various depths, including near-surface waters. This implies that there are currents *important to tracer transport* which are sensitive to f/H. It should be emphasized though that this work cannot explain *why* such steering occurs; indeed, it is not the intent to prove that the ocean acts like an unforced, barotropic fluid. Rather the goal is to document where such steering occurs, and to what extent.

Several others have examined float dispersion in the context of potential vorticity, using

Table 1. Float data and experiments. In the table, WA and EA refer to the western and eastern Atlantic respectively, Eq to the equatorial Atlantic, NP to the North Pacific and SA to the South Atlantic. The floats were also subdivided into those in the main thermocline (nominally taken to be depths ≤1000 m; referred to hereafter as "shallow" floats) and those below ("deep floats"). If a given experiment had floats at both levels, the first (second) number represents the number in (below) the thermocline.

Experiment	Reference	Location	Number
Abaco Basin	Leaman and Vertes, 1994	WA, deep	23
Brazil Basin	Hogg and Owens, 1999	SA, Eq, deep	115
Eastern Basin	Richardson *et al.,* 1989	EA, deep	25
EUROFLOAT	Speer *et al.,* 1999	EA, deep	20
Gulf Stream	Schmitz *et al.,* 1981	WA	2, 3
G. S. Recirculation	Owens, 1984	WA	26, 36
Iberian Basin	Rees and Gmitrowicz, 1989	EA, deep	6
IFM Iberian Basin	Zenk *et al.,* 1992	EA	30, 4
Kuroshio Extension	Riser, 1995	NP	53
LDE	Rossby *et al.,* 1986	WA	23, 24
Long Range	Rossby *et al.,* 1983	WA, deep	3
MODE	Rossby *et al.,* 1975	WA, deep	49
Newfoundland Basin	Schmitz, 1985	WA	9, 7
North Atlantic Current	Zhang *et al.,* 2000	WA	91, 1
Northeast Atlantic	Ollitrault *et al.,* 1988	EA, deep	14
Pre-LDE	Riser and Rossby, 1983	WA	40, 22
Ring	Cheney *et al.,* 1976	WA	5, 4
Site L	Price *et al.,* 1987	WA, shallow	33
Tropical Atlantic	Richardson and Schmitz, 1993	Eq	18, 36
Subduction '91	Joyce *et al.,* 1998	EA, shallow	16
N. Atl. Tracer Release	Sundermeyer and Price, 1998	EA, shallow	8

different methods. McWilliams (1976) used float velocities and density profiles to test the conservation of stratified quasi-geostrophic PV in the MODE region. More recently, O'Dwyer *et al.* (2000) examined the relation between float spreading and climatological PV from Levitus data, in the North Atlantic at various depths. And Bower and Hunt (2000) noted that floats below the Gulf Stream tend to follow f/H_2, where $H_2(t)$ is the depth below the thermocline. The relation of this work to the latter two is discussed at the end.

2. Data

The float trajectories were obtained from the WOCE Subsurface Float Data Assembly Center at Woods Hole (and are publicly available). These represent SOFAR and RAFOS floats, both of which are continuously tracked at depth. The float experiments, relevant references, and the number and location of the floats are given in Table 1.

The float records were divided by geographical region, and by depth (those at less than or greater than 1000 m). The records were also subdivided into shorter segments. If a tendency to drift along f/H exists, it presumedly will be observed on longer time scales, i.e.

after the Lagrangian time scale. The latter is less than 20 days in all these regions, so a 50-day record length was chosen. Because some records were much longer than this, the subdivision greatly increased the sample number and thus the statistical certainty. Records with positions recorded more frequently than once per day were averaged to produce daily records; those with less frequent positions were linearly interpolated to yield daily records. The latter was done for computational convenience and had little effect on the results. Floats in the Eastern Atlantic deployed intentionally in "meddies" (e.g. Richardson *et al.,* 1989) were excluded to avoid biases (although comments about meddies are made).

Most of the floats were isobaric, or constant pressure, and thus capable of crossing isopycnals. The divergence from actual fluid parcel paths is probably most serious in regions where the isopycnal slope is large, typically near boundaries (e.g. Riser, 1982; Davis, 1991); this is perhaps a good reason to exclude floats near boundaries. However all floats were included for the calculations so as not to bias the results. That similar results were obtained in one region which only had isopycnal RAFOS floats (the shallow northwest Atlantic, Section 4a) suggests that the isobaric floats are sufficiently representative (see also Davis, 1991).

By necessity, no distinction is made for deployment date, i.e. the ocean is assumed to be statistically stationary. The reason is a practical one: to obtain statistical significance, one must overlook the fact that the floats have been deployed over a 25 year period. While unlikely, unresolved temporal variations may also affect the results.

The topography was taken from the etopo5 set (available from the National Geophysical data center) of 5 minute gridded data, and subsampled at 10 minute resolution as part of the smoothing process. The topography was smoothed further using a spectral filtering function; the topographic data matrix was Fourier transformed, then multiplied by a function which removed smaller scales:

$$h_{smooth} = \sum_k \sum_l \hat{h}\,(k, l) \exp\,(-\alpha\kappa - ikx - ily) \tag{1}$$

where $\hat{h}$ is the transformed topography, $\kappa = (k^2 + l^2)^{1/2}$ the magnitude of the total wavevector and α a smoothing factor with dimensions of length. Such filtering mimics the effect of stratification, which causes motion to be trapped at the topography with a vertical decay scale $d \propto f\,L/N$, where N is the Brunt-Vaisala frequency (e.g. topographic waves (Rhines, 1970), or stratified Taylor columns (Owens and Hogg, 1980)). Smaller scales are more bottom-trapped, and thus less important to motion at mid-depth. With weak stratification, f/H will resemble the barotropic field, but with stronger stratification, the result will be a field intermediate between f/H and f.[2] Note that even with barotropic flows, small topographic scales are often irrelevant (e.g. Bretherton and Haidvogel, 1976; LS), so it is reasonable to filter the topography. The dependence on the level of smoothing is discussed in Section 4c.

2. A similar construct has been argued by Marshall (1995) with respect to the topographic influence on the wind-driven mean circulation.

The floats were divided into smaller subregions, in an attempt to compensate for the lateral variation of eddy kinetic energy (e.g. Wunsch, 1981). As in LS there is no decomposition into mean and eddy contributions (e.g. Davis, 1991); rather, float displacements are regarded simply as transport measurements. In most regions the mean was not well resolved by the floats. However, a mean/eddy decomposition is presented for one more densely-sampled region (Section 4b).

3. Method

The procedure for calculating the moments of displacements relative to *f/H* is outlined in LS, but reviewed briefly here. The (daily) positions were single-differenced to yield time series of zonal and meridional velocities; taking the cross/dot product with the normalized *local* gradient vectors of *f/H* yields time series of velocities along/across *f/H* (the gradient at the midpoint between the two positions was used). Then integrating the velocities yields net displacements relative to *f/H*. The mean and dispersion are:

$$M_\gamma(t) = \frac{\sum_i (\gamma_i(t) - \gamma_i(0))}{N} \pm z\left(\frac{D_\gamma(t)}{N-1}\right)^{1/2}, \tag{2}$$

and

$$D_\gamma(t) = \frac{\sum_i (\gamma_i(t) - \gamma_i(0) - M_\gamma(t))^2}{N-1}\left[1 \pm z\left(\frac{2}{N-1}\right)^{1/2}\right]. \tag{3}$$

where γ is the displacement, N the number of measurements and $z = 1.96$ at the 95% confidence level (the displacements are assumed to have a normal distribution).

Higher moments, such as the skewness or kurtosis, can also be computed. In fact, the skewness is sometimes useful for evaluating advection by a mean (LS); more often though, the results are less clear cut. So we concentrate only on the first two moments hereafter.

The value of α for smoothing the topography (relation 1) was fixed at 6×10^4 m. This corresponds to a length scale of roughly $\alpha/\pi \approx 20$ km. For the stratified Taylor column, $L_z \propto \exp(-N\,d\,\kappa/f)$, so $\alpha = N\,d/f$. This could be obtained with a mean depth of 3000 m from the bottom, and a ratio of *N/f* of 20 (or similar combinations with the same product). This value produced the "best" results, as discussed in Section 4C.

As discussed in LS, projecting float displacements onto *f/H* does not conserve distance, because *f/H* is usually curvilinear. An extreme example of this is when floats move around closed *f/H* contours, because the displacement along *f/H* increases without bound though the absolute displacement does not. In such cases, there are large differences between the moments relative to *f/H* and the standard (geographical) moments. Though one does not find similar examples with these floats, still the distance is not conserved and one must view the magnitudes of the (*f/H*) moments accordingly. As stated, the value of this approach is in detecting preferences in the direction of spreading.

4. Results

a. North Atlantic

The North Atlantic floats are considered first, with results shown in Figures 1 to 7. The floats have been subdivided into four subsets: northeast, southeast, northwest and southwest. At the shallower level there are very few floats in the northeast region, so only three subsets are considered.

The plot format is the same in all cases. In the upper panel is the smoothed version of f/H with the relevant trajectories superimposed. At lower left are the mean zonal and meridional displacements, as well as those along and across f/H. At the lower right are the dispersions in the four directions. The 95% confidence limits are indicated for the means and dispersions relative to f/H only, and are indicated by small dots. The displacements have not been normalized (Rupolo *et al.,* 1996), and so represent real distances. Non-normalized distances were chosen to facilitate comparisons of dispersion from region to region.

In the following examples, we will be primarily concerned with whether the mean advection or dispersion is anisotropic or not. "Anisotropic" thus signifies that one component (along or across f/H, or in the zonal or meridional direction) is greater than the other. Thus "weak zonal anisotropy" suggests the zonal direction is preferred over meridional, and "anisotropy along f/H" implies spreading across f/H is less.

The 259 50-day trajectory segments in the deep northwestern Atlantic (Fig. 1) are in a region of nearly zonally-oriented f/H contours, except for those near the continental slope. In the interior, the gradient of f/H is weak and dispersion substantial. Near the slope, the trajectories are more confined. The means (lower left panel) are not significantly different from zero in any direction; thus despite that many of the floats were below the Gulf Stream, there is no apparent tendency east or west (see also Owens, 1991). The dispersion is slightly more zonal than meridional, but the dispersion along f/H is greater than in the zonal direction, and the dispersion across f/H is less than in the meridional direction. Thus greater anisotropy with respect to f/H is indicated. With only the floats in the interior region, the zonal and along-f/H dispersion are nearly the same, but the floats near the boundary are steered by the slope which is accounted for by the f/H projection. Note the dispersion increases approximately linearly after about 10 days in all directions, consistent with diffusive spreading after the Lagrangian integral time (Taylor, 1921; Batchelor and Townsend, 1953).

The 416 trajectories in the southwestern part of the domain (Fig. 2) display similar dispersion characteristics: weak zonal anisotropy, but greater along-f/H anisotropy, and diffusive spreading after about 10 days. The dispersion is less than in the previous set, suggesting weaker rms variability. The means are not significantly different from zero in the zonal or cross-f/H directions, but they are in the meridional and along-f/H directions, and suggest a southward drift at about 1 cm/s. This is probably due to advection by the deep western boundary current (e.g. Owens, 1991). Note the dispersion is zonally enhanced and the mean drift meridional, whereas both mean and dispersion are enhanced along f/H.

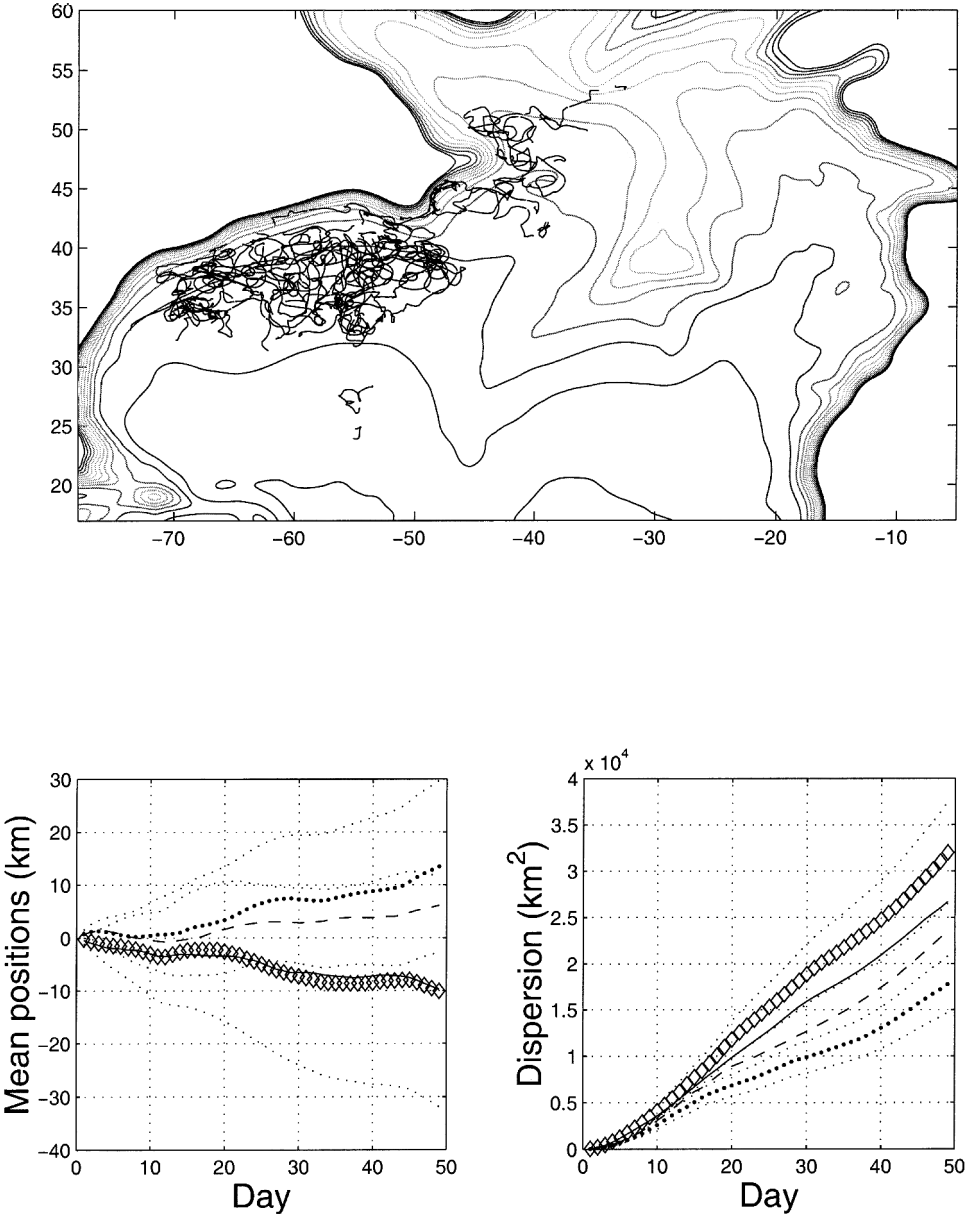

Figure 1. Floats in the northwestern North Atlantic below 1000 m. The trajectories, superimposed on the smoothed *f/H* contours, are shown in the upper panel. The contour values for *f/H* are [5 10 15 . . . 70] $*$ 1 $\times$ 10^{-9} $(ms)^{-1}$. In the lower panels are the mean displacements (left) and the dispersions for the set; the solid lines are for zonal displacements, dashed for meridional, diamonds for along *f/H* and dots for across *f/H*. The small dots indicate the 95% confidence limits for the along and across *f/H* quantities.

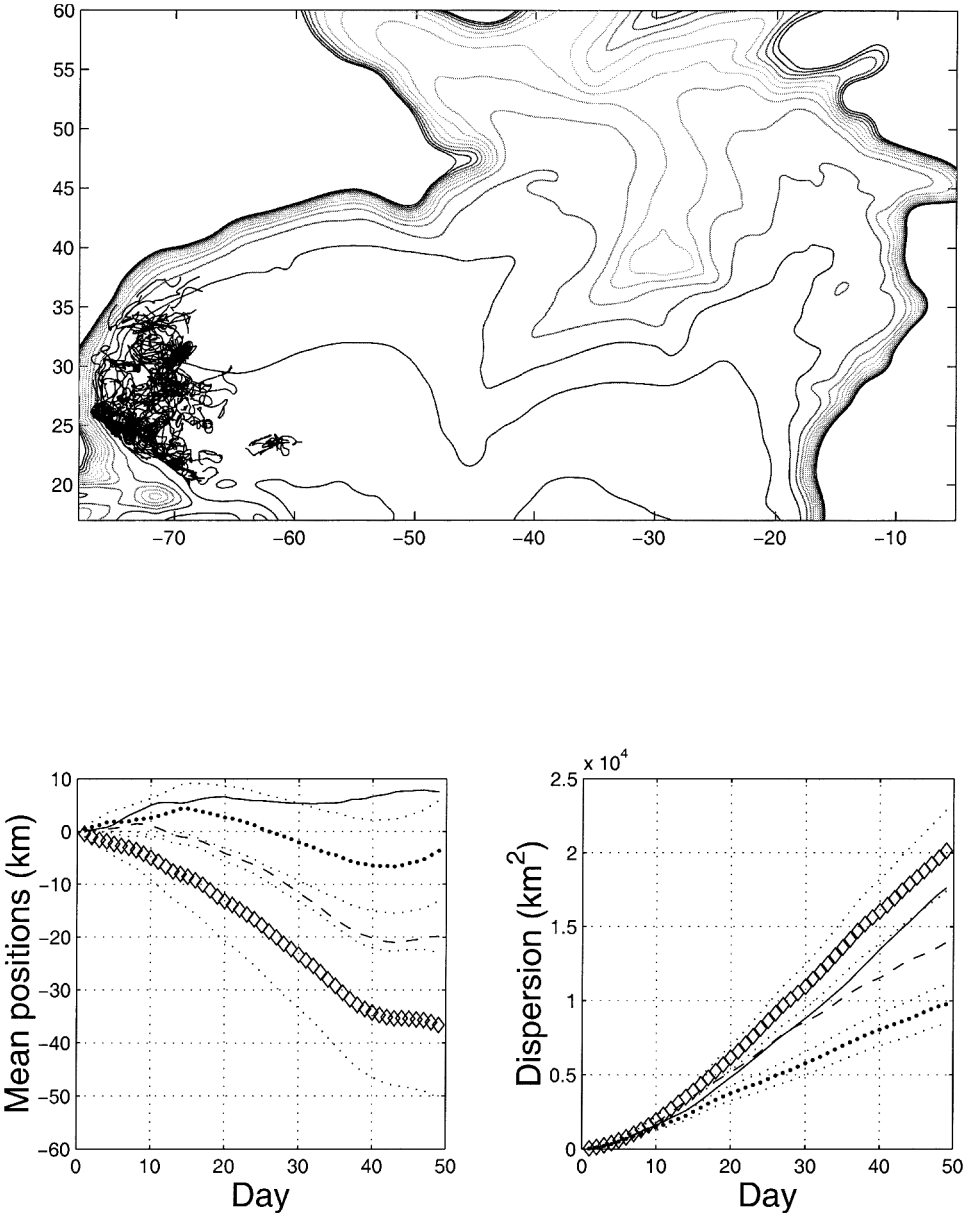

Figure 2. Results for floats in the southwestern North Atlantic below 1000 m. The *f/H* contour values and the symbols are as in Figure 1.

In the southeast there are 273 trajectories (Fig. 3), most of which come from the Eastern Basin float experiment (Richardson *et al.,* 1989). The dispersion here is roughly half as great as in the west, reflecting weaker eddy kinetic energy. The statistics of these floats were discussed previously by Spall *et al.* (1993), who noted in particular the preference for

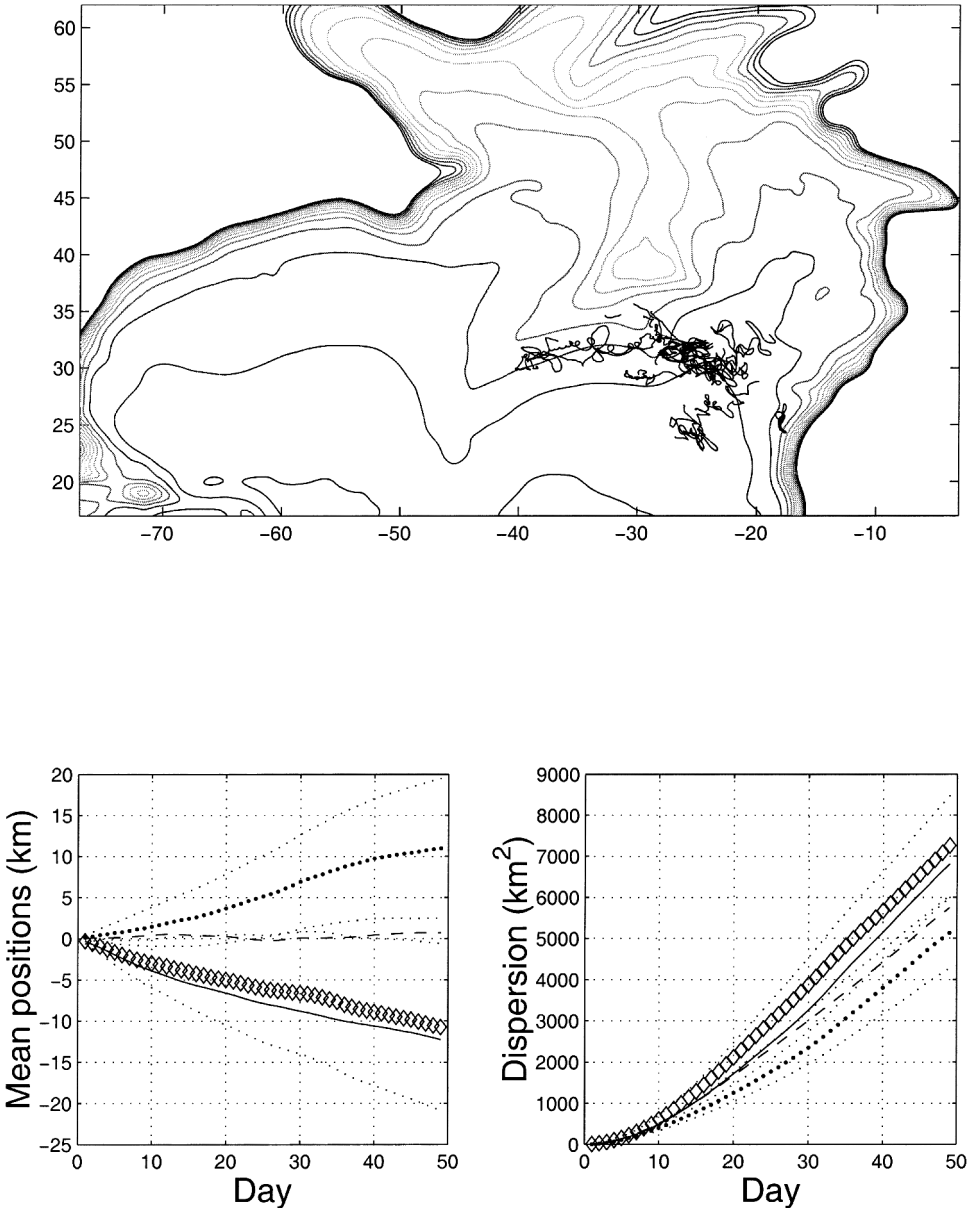

Figure 3. Results for floats in the southeastern North Atlantic below 1000 m. See Figure 1 for details.

zonal spreading. Anisotropic spreading is also evident here, and because *f/H* is largely zonal in this region (Fig. 3), the mean drift and dispersion along *f/H* is not significantly different from that in the zonal direction. Note the dispersion within the errors increases linearly at late times, but only after roughly 20 days, indicating a longer Lagrangian time scale (also noted by Spall *et al.,* 1993).

The means suggest a weak westward movement at roughly 2 mm/s. There is no net meridional drift,[3] but there is a weak but significant drift *up f/H*. On closer inspection, the latter is found to be related to a number of floats threading between the Cruiser and Great Meteor seamounts (near 30N, 30W), which have been smoothed out. Many of these floats actually turned southwestward, back along *f/H*, but only after the 50-day time period. So the process of breaking up the trajectories contributes to this apparent drift.

The 382 trajectories in the northeastern region (Fig. 4) are primarily from the EURO-FLOAT experiment (Speer *et al.,* 1999). The statistics here contrast interestingly with those in the southeastern region. Whereas strong zonal anisotropy was found there, here the geographic dispersion is *isotropic*. However, projecting the displacements onto *f/H* alleviates the discrepancy, for here too the dispersion is greater along than across *f/H*. The reason for the difference between this region and the Eastern Basin is probably the mid-Atlantic ridge which deforms *f/H* much more in the northern portion of the domain. The only mean significantly different from zero is that along *f/H*; it reflects a slow drift to the pseudo-west (in the sense that larger values of *f/H* lie to the right).

While perhaps unsurprising that topography influences floats in the deep ocean, similar results were obtained with the shallower floats in the North Atlantic. Consider the 441 trajectories in the upper 1000 m of the northwestern Atlantic (Fig. 5). Most of these lie in the region between the continental slope and the ridge; while some successfully navigate around the ridge to the north, few cross directly over. It is true that most floats were deployed close to the western boundary and that many ended their lifetimes before reaching the ridge, but the vast majority of floats from another experiment in the same region (the TOPOGULF experiment: Ollitrault, 1995) were also apparently blocked by the ridge. In addition, the stochastic model floats described in Section 4d, deployed in the same locations as the northwestern Atlantic floats and with equal lifetimes, were unaffected by the ridge.

The shallow northwestern Atlantic set provides the clearest evidence for control by *f/H* of any in the present work. The dispersion, which is meridionally enhanced, is much greater along *f/H* than in any other direction. The rapid mean drift along *f/H*, of order 3.5 cm/s, is significantly greater than in any other direction, and the drift across *f/H* is essentially zero. The geographical mean is northwestward, consistent with advection by the North Atlantic Current (Zhang *et al.,* 2000). The present results thus imply the NAC is largely oriented along *f/H* (see also Section 4b). The implied sensitivity of these floats to the topography is striking, given that their mean depth is only 500 m.

The set from the upper southwestern Atlantic has 453 trajectories and covers a broad area (Fig. 6). As in the northwestern region, the mean is largest along *f/H* and corresponds to a speed of just under 1 cm/s; the other means aren't different from zero at the 95% level, even the zonal mean which is weakly eastward. The zonal dispersion is nearly three times greater than the meridional dispersion. Many of the floats were deployed in the Gulf

3. Recall that floats in meddies have been excluded. There *is* a net southward drift when they are included; see also O'Dwyer *et al.* (2000).

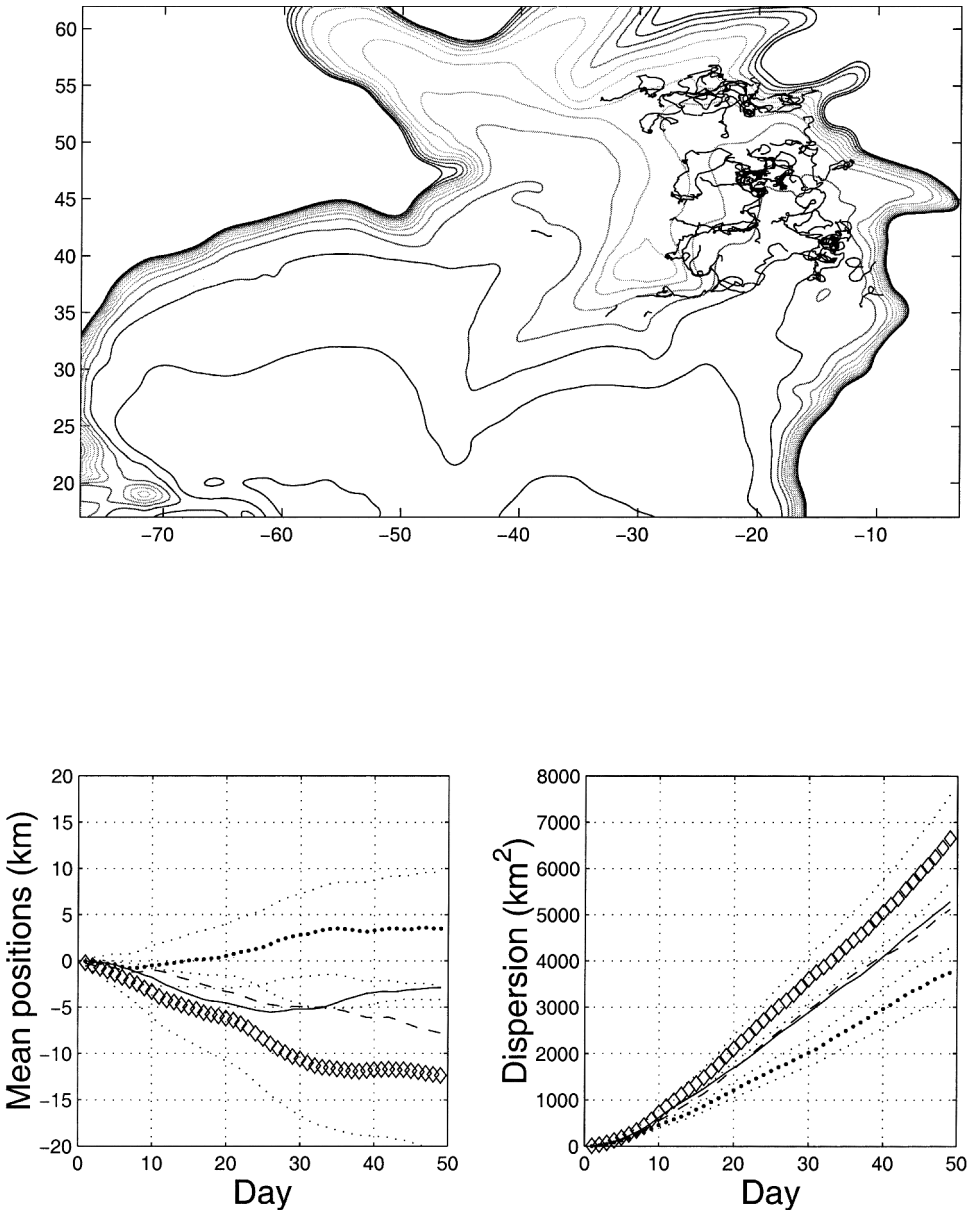

Figure 4. Results for floats in the northeastern North Atlantic below 1000 m. See Figure 1 for details.

Stream, and it is interesting that so few exhibit steady, jet-like advection (the Gulf Stream is evident only after binning the data geographically, as in Section 4b). The impression instead is one of strong, zonally-enhanced mixing. The dispersion along *f/H* is *equal* to the zonal dispersion, and likewise the dispersion across *f/H* is only somewhat smaller than in

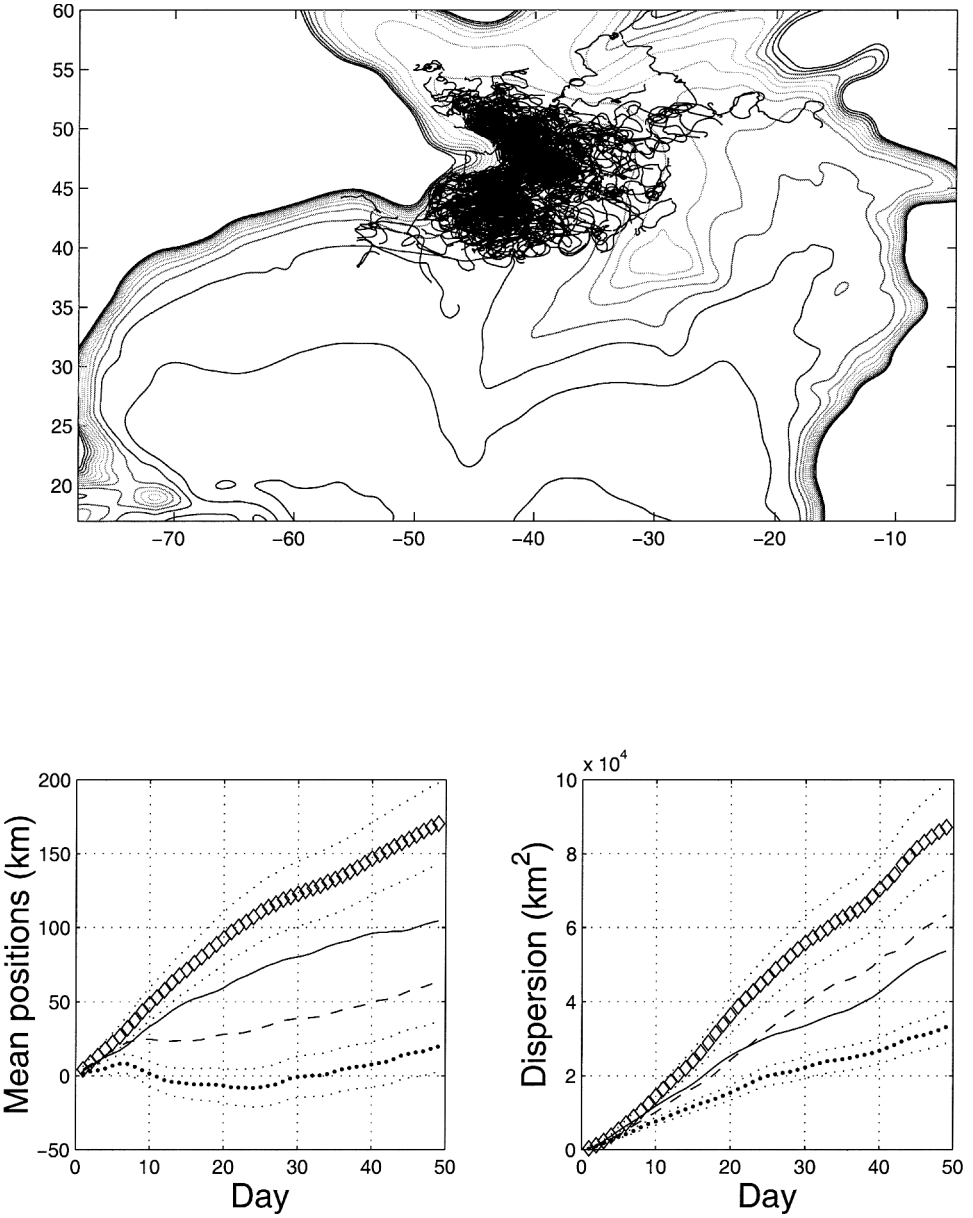

Figure 5. Floats in the northwestern Atlantic above 1000 m depth. See Figure 1 for details.

the meridional direction. The dispersion occurs primarily in the interior, where *f/H* is nearly zonal; in contrast, mean advection apparently happens primarily near the boundary, where *f/H* is not zonal.

The last set in the upper North Atlantic are the 211 trajectories in the east (Fig. 7). Many

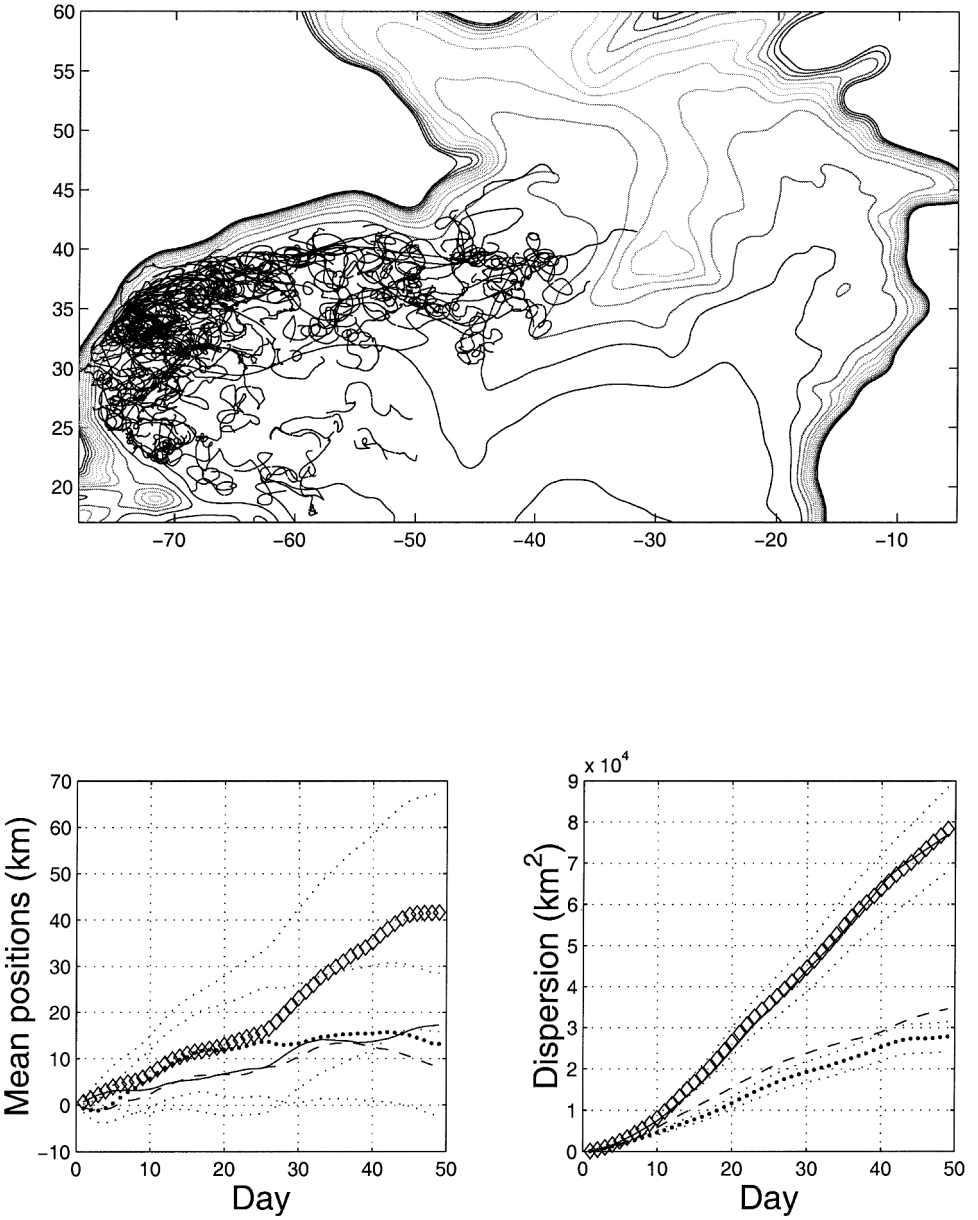

Figure 6. Floats in the southwestern Atlantic above 1000 m depth. See Figure 1 for details.

of the trajectories lie near 25W, 25N and off the Iberian Peninsula, where the gradient of *f/H* is weak. The shallow eastern set stands out, because the dispersion is isotropic at the 95% confidence level in both geographical and *f/H* coordinates. And while the zonal mean drift and that along *f/H* are not different from zero, there *is* a significant drift southward (and

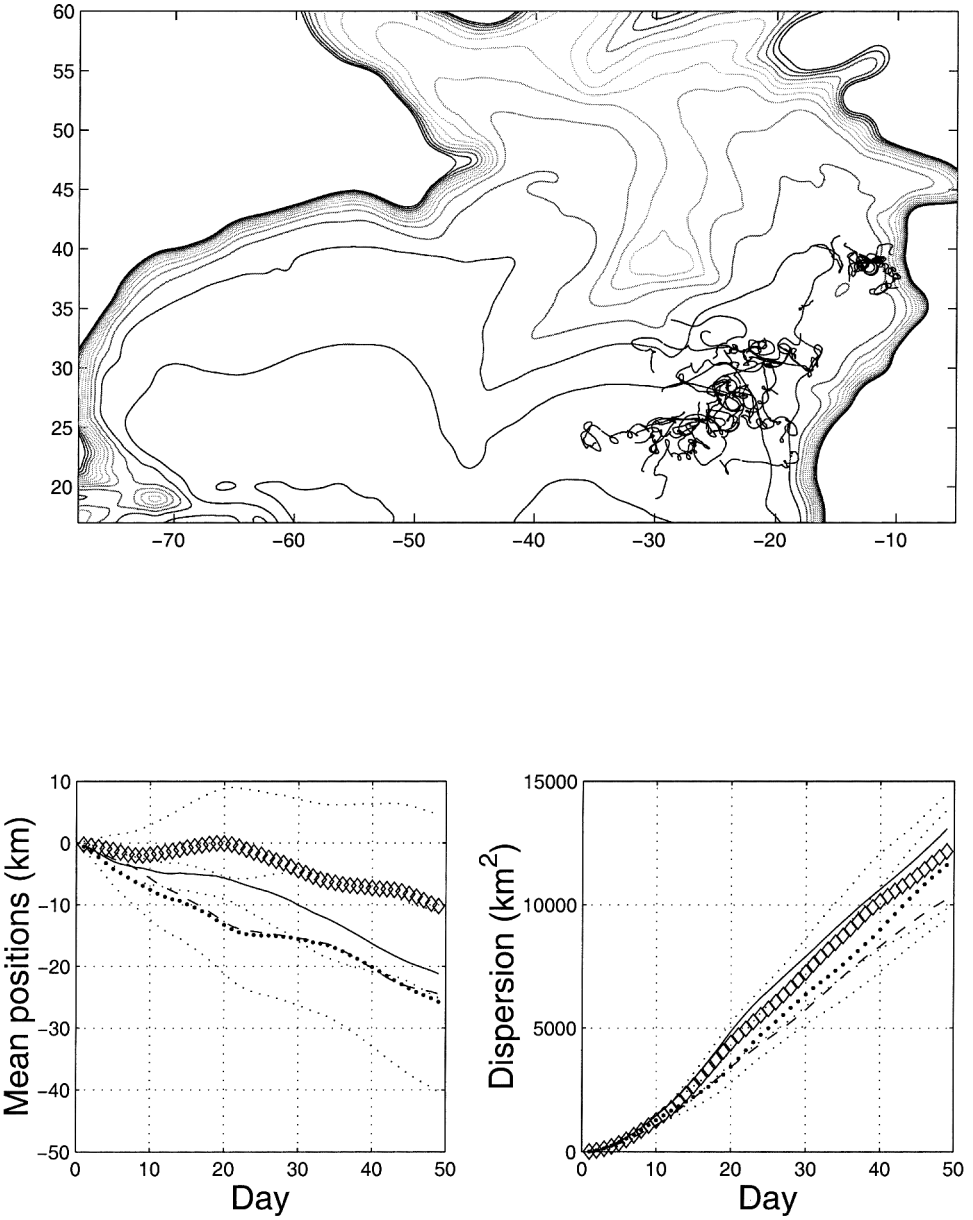

Figure 7. Floats in the eastern Atlantic above 1000 m depth. See Figure 1 for details.

across f/H) which corresponds to a speed of roughly 5 mm/s. Were the ocean barotropic, the indication would be that PV is not conserved. In fact this is true for at least a portion of the floats; the (quasi-isopycnal) floats in the Subduction experiment were observed to move southwestward, consistent with advection by the wind-driven Sverdrup flow (Joyce *et al.,* 1998).

In fact, it is perhaps more notable that no mean drift across *f/H* is found in the shallow western North Atlantic. One possible explanation is that directly-forced currents there may be much weaker than variable, PV-conserving currents, such as eddies generated by the baroclinically unstable Gulf Stream. However, given only this data one can only speculate (see also below).

Thus we find evidence that Lagrangian transport and mixing are sensitive to topography in the North Atlantic, throughout the water column. The one exception is the shallow Eastern Atlantic, where floats exhibit a significant drift across contours, perhaps because of wind forcing. Before examining floats in other basins, several related issues are discussed: the decomposition into the (Eulerian) mean and eddy fields, and the effect of varying topographic resolution. In addition, a test case with a collection of model-generated trajectories oblivious to *f/H* is also considered.

b. Mean-eddy decomposition

Ideally, one would separate the mean and eddy contributions (e.g., Davis, 1991) and discuss how each relate to *f/H*. The density of data in the shallow western North Atlantic makes this the region best-suited for such a calculation.

To determine the means, the daily velocities were collected in geographical bins and averaged. For the following example, one degree square bins were used, and only those bins with more than 30 realizations were taken (otherwise the mean was set to zero); no "array bias correction" was made (Davis, 1991). Binning velocities does not preclude a single float determining the mean in a bin, implying the results may reflect Lagrangian more than Eulerian drift in some cases. However, if the sampling is dense enough the binned mean is often a reasonable proxy for the Eulerian. More sophisticated techniques exist, for instance objective analysis (Davis, 1998), but for simplicity only the binned means were used. For a complete discussion of the procedure and related issues, see Davis (1991).

Given the Eulerian mean, one may interpolate to find the value at a given float position. Thus at any time, the float has an associated mean velocity and a residual, and both can be projected along and across *f/H*. Integrating the velocities as before yields equivalent mean- and eddy-induced displacements.

All the floats in Figures 5 and 6 were used, and the resulting mean flow is shown in Figure 8. The Gulf Stream is seen separating from the American coast at Cape Hatteras, and the North Atlantic Current on the western side of the Newfoundland basin (see Owens, 1991 and Zhang *et al.,* 2000). One frequently observes the mean following *f/H*, but there are exceptions too, such as where the Gulf stream separates, and in regions where the gradient of *f/H* is weak. The "Mann Eddy" (Rossby, 1998) lies in such a region, near 42N, 45W.

The displacement moments are shown in Figure 9. The mean displacements due to the residuals (upper right panel) are essentially not different from zero, suggesting the mean flow has been captured by the binning process. The mean flow (upper left panel) is to the

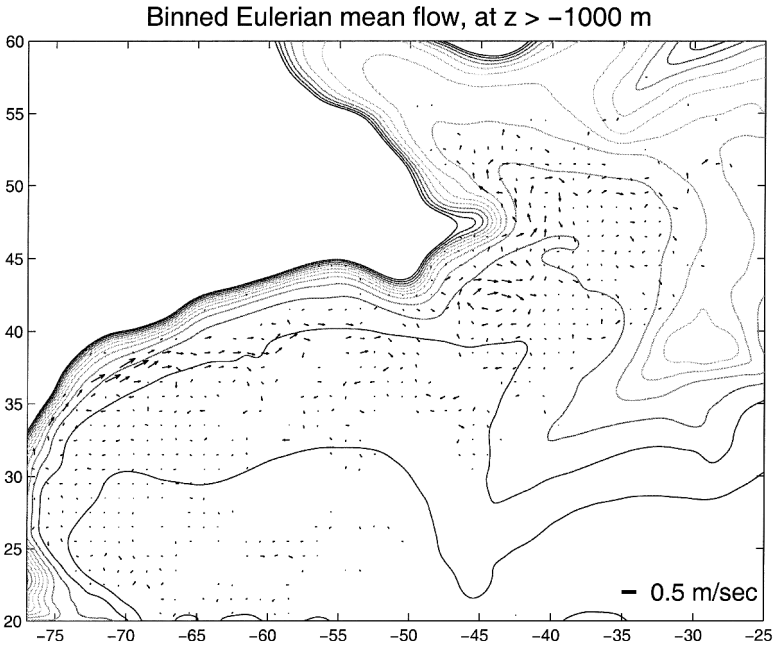

Figure 8. Mean velocities derived from floats in the shallow western North Atlantic superimposed on *f*/*H*. Float velocities were binned in one degree squares, and only bins with more than 30 realizations were used. The velocity scale is indicated in the lower right corner.

northeast, but is more clearly oriented along *f*/*H*, with the displacement along contours 50% greater than in the zonal direction. There is a faint suggestion of a drift *up f*/*H* as well. However the cross-*f*/*H* drift magnitude varies with topographic resolution. It also changes if two rather than one degree square bins are used (unlike the along-*f*/*H* or geographical drifts). So the mean displacement across *f*/*H* may be related to floats crossing smoothed contours. If the drift actually exists, it would reflect slow poleward movement.

The mean (which has significant horizontal shear, Fig. 8) induces dispersion. The geographical dispersion due to the mean is isotropic within the errors, but the dispersion is strongly anisotropic with respect to *f*/*H*. In all directions the mean-induced dispersion increases more rapidly than linearly, although less than quadratically, as one would expect for a unidirectional shear flow (e.g. Taylor, 1953). Like the mean-induced dispersion, the eddy dispersion appears isotropic in (x, y), but is strongly anisotropic with respect to *f*/*H*. In contrast, the eddy-induced dispersions are approximately twice as great and are increasing linearly, within error.

Comparing these results with the purely Lagrangian ones (Figs. 5 and 6), we observe that the decomposition relegates the bulk of the mean drift to the (Eulerian) mean and the dispersion to the eddies. Arguably the most interesting aspect is the comparison between the mean- and eddy-induced dispersions. The mean/eddy decomposition was performed in

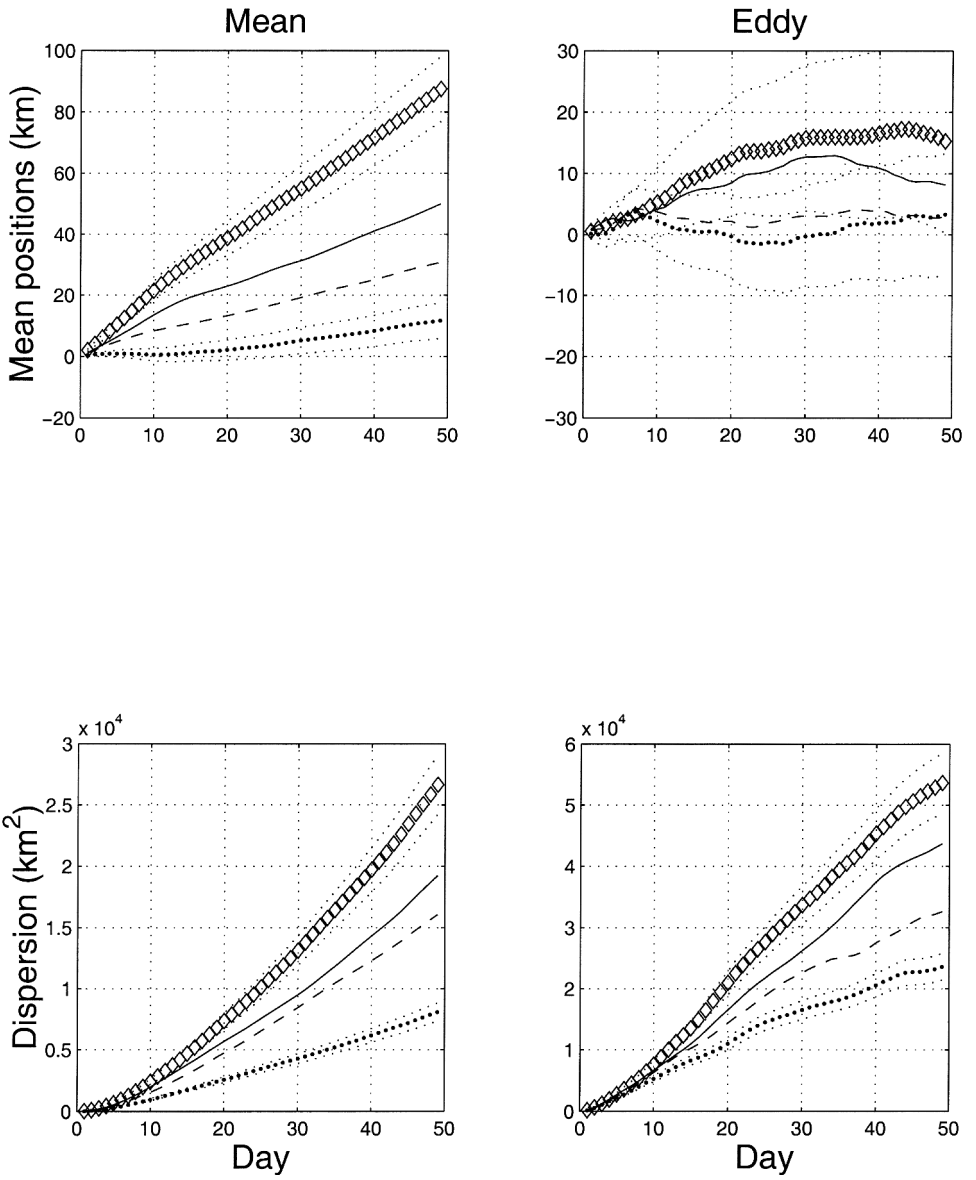

Figure 9. Results for the floats in the western North Atlantic above 1000 m depth, following a decomposition of the velocities into mean and eddy components. The mean flow statistics are on the left, and the eddy statistics on the right. See Figure 1 for symbol labels.

all the other regions as well, with a similar relegation, so no significant new information is gained by presenting other cases.

There are good reasons (e.g. Davis, 1991) to identify that portion of the dispersion due to the time-varying portion of the flow. However, the sense here is that such a decomposition

would be greatly improved with either much more float data, or an independent determination of the Eulerian mean. Such things could be done in the future.

c. Topographic resolution

As noted in Section 2, the topographic filtering parameter, α, was chosen to yield the best results. In fact, the results do not depend strongly on topographic resolution, but changes are apparent when the topography is either too noisy or over-smoothed. Here we consider three sample calculations with the shallow northwestern Atlantic floats under various levels of topographic smoothing.

The calculations were made with $\alpha = 6 \times 10^3$, 6×10^4, and 6×10^5 m (corresponding to smoothing scales of 2, 20 and 200 km). With $\alpha = 6 \times 10^3$ m, many of the small scales are retained, as shown in Figure 10. With $\alpha = 6 \times 10^5$ m, f/H is zonal in most regions. In analogy to a stratified Taylor column, a low value of α corresponds to being near the bottom or having weak stratification, and a large α to strong stratification or a position far from the bottom.

The $\alpha = 6 \times 10^4$ m calculation yields the largest mean drift and dispersion along f/H (Fig. 11). The means and dispersion along f/H are less for both the high and low resolution topography cases. If f/H is too noisy, the gradients obtained from differencing are even noiser, and the process of projecting displacements is impaired. (A detailed discussion of error accumulation is presented in LS.)

If the topography is too smooth, the moments along/across f/H approach those relative to (x, y) because f/H is more zonal. Though over-smoothing appears to impact the along-f/H dispersion as much as does under-smoothing (lower left panel), the effect on the mean is less pronounced (upper left panel). This suggests that the mean is less sensitive to details in the topography than are the eddies, but one could only speculate about the reason for this.

It is significant that the dispersion across f/H is lowest with $\alpha = 6 \times 10^3$ m, i.e. the noisy topography case. Most likely this is related to the accumulation of errors which affects the dispersion more severely than the mean (LS). In any case, a small cross-f/H dispersion alone is not a good indication of anisotropic spreading. A more robust measure appears to be the increase in the along-contour dispersion.

d. Stochastic trajectories

If the present method is capable of distinguishing whether dispersion is sensitive to topography, likewise it ought to be able to tell when it isn't; for instance, with particles undergoing a random walk. This suggests a null hypothesis test, which was carried out by means of a numerical calculation. A routine was written to generate stochastic trajectories from the same starting positions as the floats in the six previous sets. Their velocities were then projected onto f/H, and the means and dispersions compared with the actual floats. Stochastic "floats" experience diffusive spreading after the Lagrangian time scale, as do the real floats (see above), and their geographical statistical moments can be tuned by

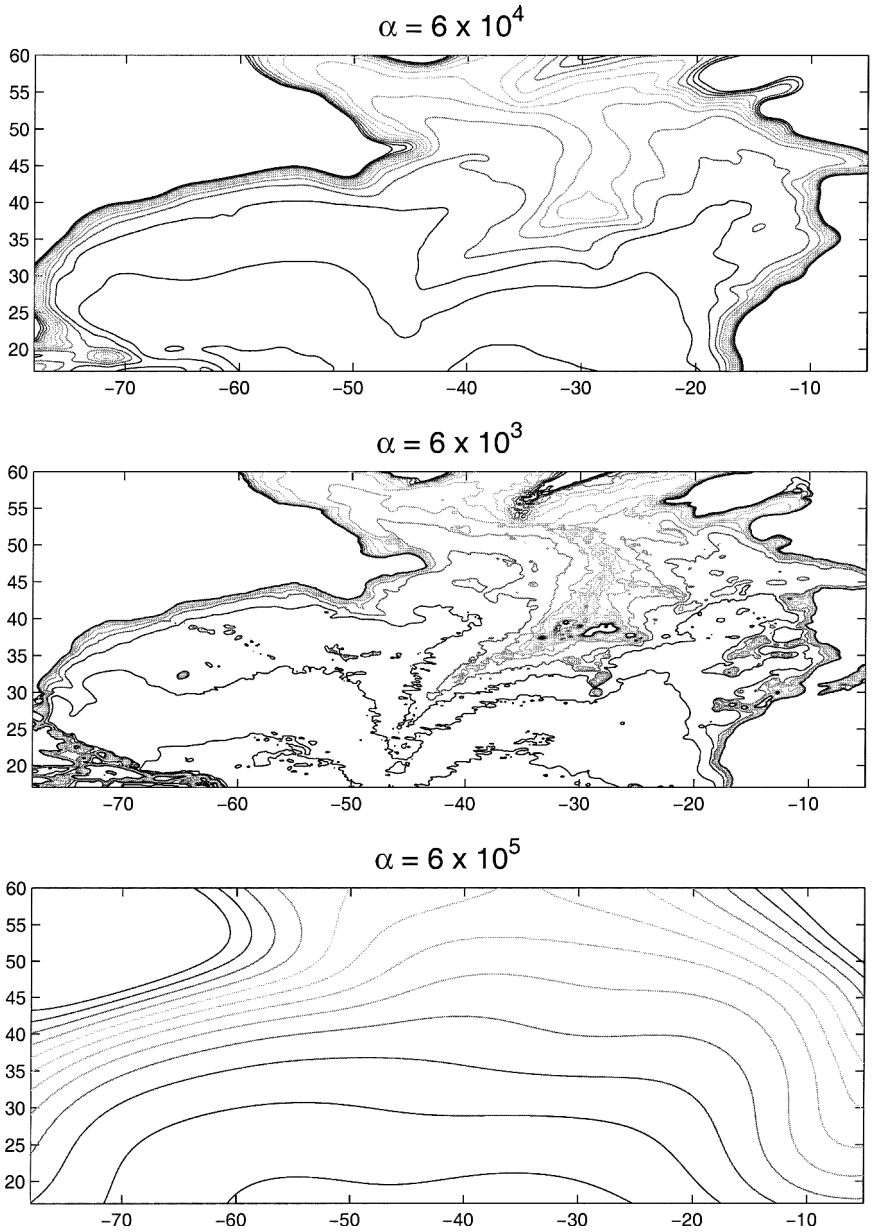

Figure 10. *f/H* with various degrees of smoothing. The topography, which is of 10 minute resolution, has been smoothed with a wavenumber filter $\propto \exp(-\alpha\kappa)$. In the upper panel is *f/H* with $\alpha = 6 \times 10^4$ m, whereas the middle panel corresponds to $\alpha = 6 \times 10^3$ m and the lower to $\alpha = 6 \times 10^5$ m. The contour values are as in Figure 1.

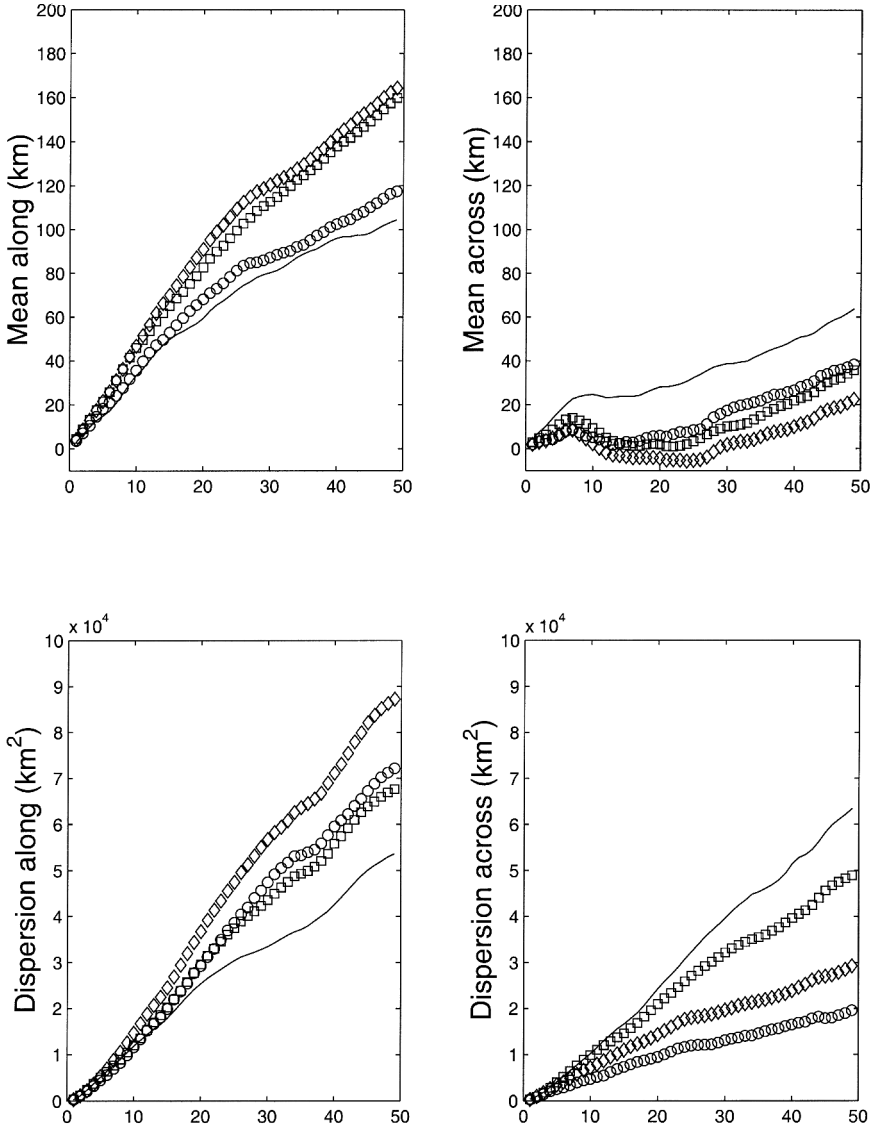

Figure 11. Displacement statistics for the floats in the shallow NW Atlantic with variously smoothed topography. The diamonds correspond to $\alpha = 6 \times 10^4$ m, the circles to $\alpha = 6 \times 10^3$ m and the squares to $\alpha = 6 \times 10^5$ m. The solid lines indicate the geographic displacements.

adjusting parameters of the model. A good discussion of matching stochastic models to data can be found in Griffa *et al.* (1995).

The trajectories were generated by numerically integrating the following deterministic position equations:

$$dx = (u + \overline{U})\, dt, \qquad dy = (v + \overline{V})\, dt, \tag{4}$$

and Markovian equations for the velocities,

$$du = -\frac{1}{T_x} u dt + n_x dW, \qquad dv = -\frac{1}{T_y} v dt + n_y dW, \tag{5}$$

(e.g. Sawford, 1993; Griffa *et al.,* 1995), where $\overline{U}, \overline{V}$ are the mean zonal and meridional velocities, dW is the incremental Wiener process (Gaussian with zero mean) and T_x and T_y the Lagrangian time scales in the zonal and meridional directions. The noise amplitudes, n_x and n_y, as well as the Lagrangian time scales, were chosen to yield zonal and meridional dispersions as close as possible to the observed values for the corresponding float set. The mean velocities likewise were adjusted to produce comparable mean drifts. A few "floats" which moved into less than 100 m of water were discarded, but this did not affect the group statistics.

The results of the stochastic "deployment" in the northwestern Atlantic are shown in Figure 12; as noted, the initial positions were the same as those in Figure 5.[4] There are visual similarities with the actual trajectories, due in part to the relatively short record length, but there are differences too. Inspection reveals that these floats are more likely to spread over topography than their aquatic counterparts, and in the region of the mid-Atlantic ridge in particular.

The latter difference is clearly evident in the projected displacement moments. While the zonal and meridional means are similar by design to those in Figure 5, the mean along *f/H* is smaller. Furthermore the net drift across *f/H* is not statistically different from that along *f/H*.

The geographic dispersions are seen to be similar to those in Figure 5, but the dispersion relative to *f/H* is *isotropic,* and smaller than either the zonal or meridional dispersion. So the moments suggest no statistical sensitivity to *f/H*.

Note the point here was to examine a set of floats with no sensitivity to *f/H*. We could have obtained a better correspondence between the stochastic and actual floats by using a spatially variable mean and diffusivity. Indeed, with fine enough resolution one could presumedly mimic the sensitivity to *f/H*. But such trajectories would have been of little use for testing the method.

Similar results are found in the other five regions of the North Atlantic, i.e. the stochastic

4. Note that the stochastic floats were launched at locations corresponding to the beginning of the 50-day float segments in the northwest. An alternate method would be to generate longer trajectories, then break those into 50-day segments. However, the present approach better facilitated the matching of statistics.

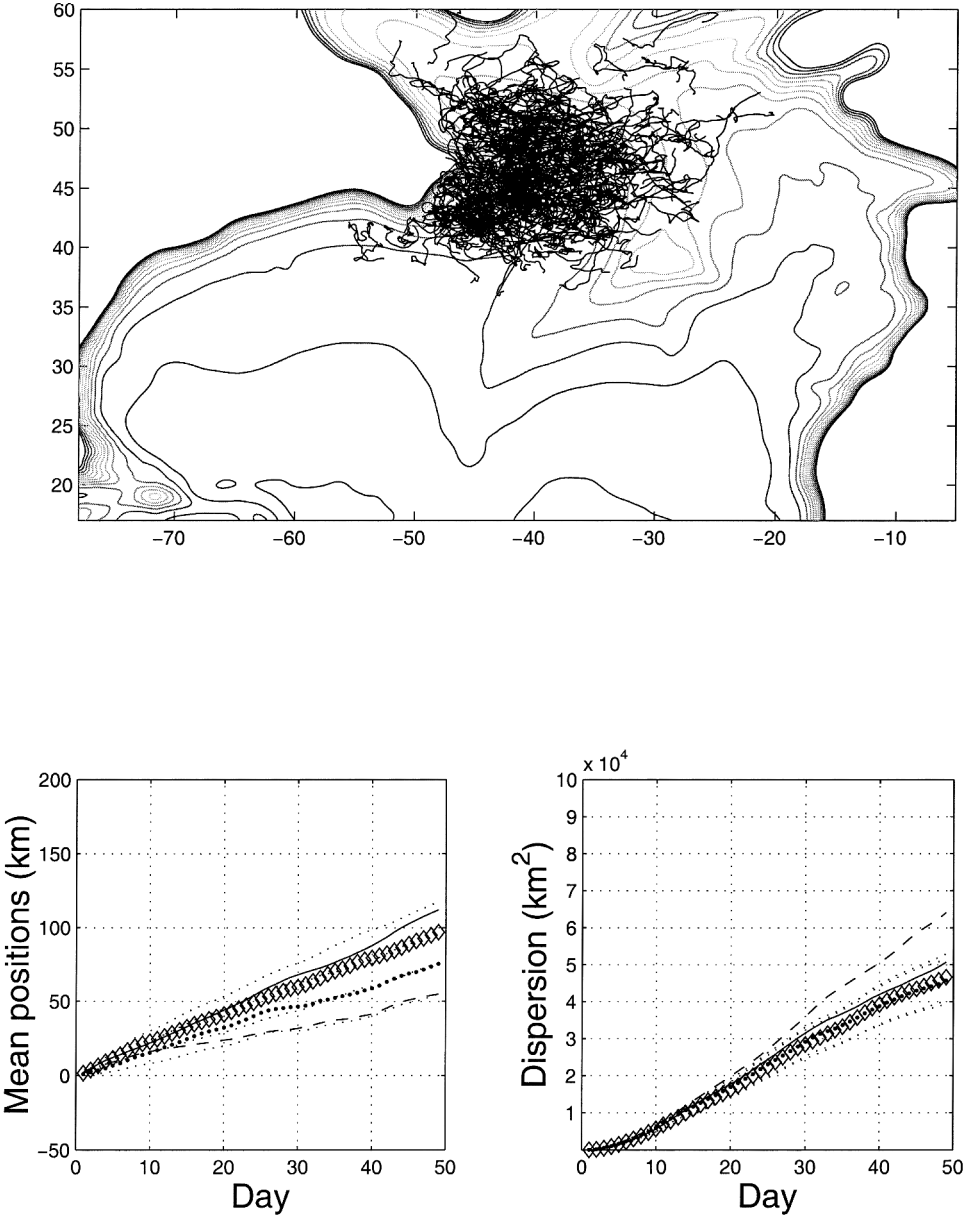

Figure 12. Stochastic particle trajectories in the northwestern Atlantic region. The particles began at the same locations as the actual floats in the region, and have similar zonal and meridional dispersion characteristics (see text).

floats tend to drift as much across f/H as along it, and the dispersion is always less than the maximum of the meridional or zonal dispersions. Of course this negative result does not prove that the actual floats are sensitive to f/H, but it is at least consistent with that notion.

e. Equatorial Atlantic

Most of the data in this region comes from the Tropical Atlantic Experiment (Richardson and Schmitz, 1993); additional equatorial trajectories from the Deep Basin Experiment (Hogg and Owens, 1999) were also included. Most were at depths from 800 to 2000, although some were deeper; given this, and the relatively small number of trajectories, all were taken together for the calculations.

The region can be characterized as a relatively flat interior and a western boundary, and the floats were subdivided accordingly. The "interior" floats are shown in Figure 13. Many exhibit long zonal paths, with north-south oscillations superimposed, whereas others (those near Africa and some near 10N, 45W) are more stationary. The f/H contours are essentially zonal over most of this region.

The statistics suggest zonal (and thus along-f/H) anisotropy. The zonal dispersion is more than four times greater than the meridional, and moreover is increasing faster than linearly in time, with $D_{zonal} \approx D_{\|f/H} \propto t^{1.6}$. The meridional and cross-f/H dispersion are equal within error, and increasing linearly in time. Interestingly, the means are not different from zero in any direction, so eastward drifts are as likely as westward drifts. This could be the result of advection by the equatorial currents and countercurrents, but also could be due to wave advection (Flierl, 1981; LS).

The "boundary" trajectories are shown in Figure 14. Because many floats cross the equator, they also cross f/H contours. Therefore, statistics were also calculated for displacements relative to a similarly smoothed version of the topography alone. The f/H, H and geographical moments are shown in the lower panels.

The dispersion along f/H is less than the zonal dispersion. However, this is due to the equator crossing because the dispersion along the isobaths is greater than either. The meridional dispersion exceeds the cross-f/H dispersion, but the dispersion across isobaths is lower still (again due to the equator crossing). The rate of increase in the dispersions is not constant, but is also not different from linear within the errors.

The means suggest a positive drift along f/H and to the east, but a negative drift along the isobaths (a consequence of the depth increasing away from the boundary). In all three cases, the corresponding velocity is order 1 cm/s. The other means are not different from zero. Some of the floats at 1800 m are moving south with the North Atlantic Deep Water (Richardson and Schmitz, 1993), and indeed there is a net drift to the southeast for the 1800 m float subset. But the shallower floats, many of which are north of the equator, exhibit no net meridional drift.

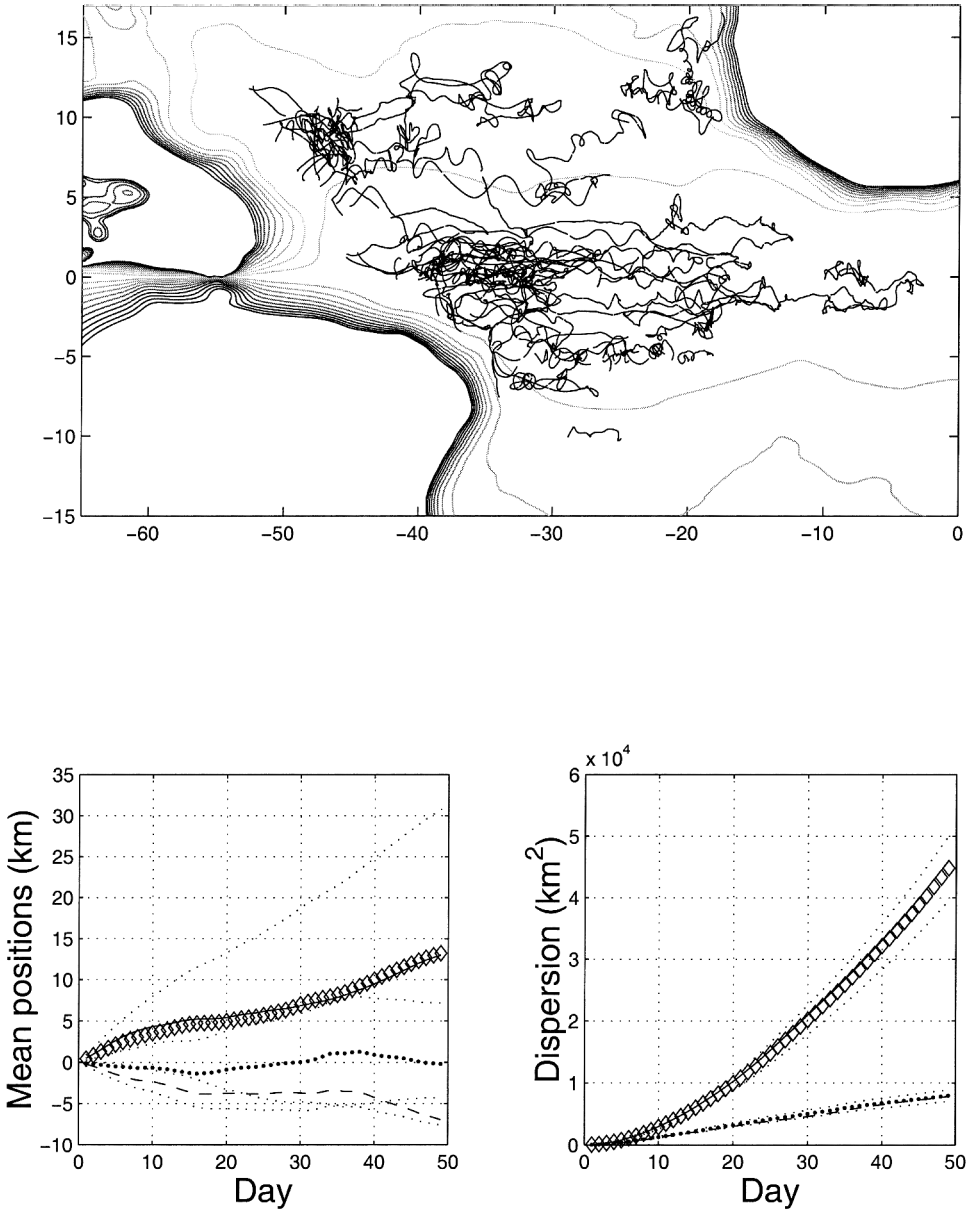

Figure 13. The results for the floats in the interior region of the equatorial Atlantic. The depths range from 800 to 3300 m. The contour values for f/H are [3 6 9 . . . 30] $*$ 1 $\times$ 10^{-9} $(ms)^{-1}$, and the moment symbols are as in Figure 1.

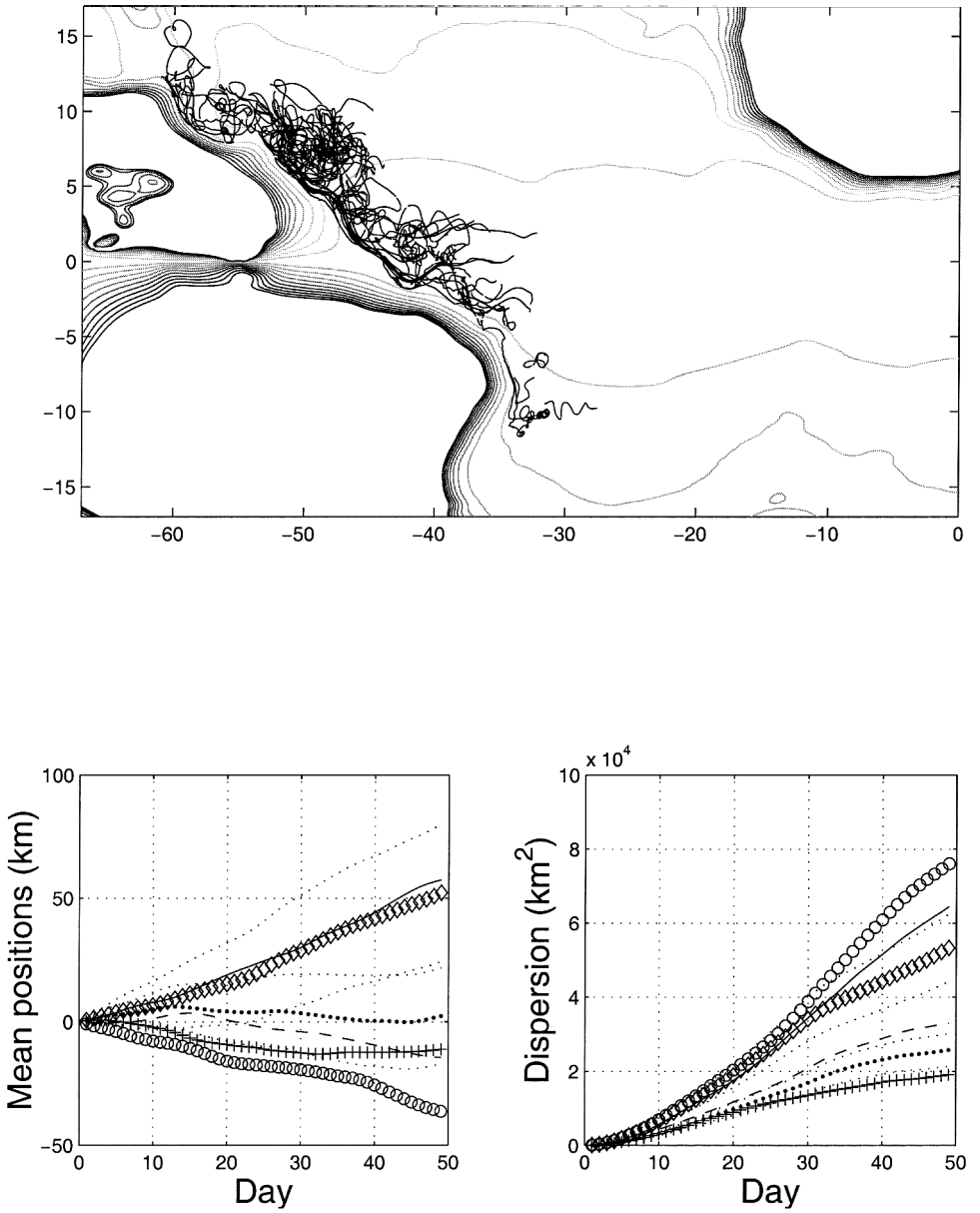

Figure 14. The results for the floats in the boundary region of the equatorial Atlantic. The contour values are as in the preceding figure. The moment symbols are as in Figure 1, with the addition of moments along *topography* (circles) and across topography (plusses).

The fact that floats cross the equator (and thus f/H) reminds us that dissipative processes are often important for boundary currents, so it is unreasonable to expect PV conservation. Nevertheless the floats there still follow the isobaths. The same comment applies near the western boundary in the North Atlantic, but since topography dominates f/H near boundaries and f is nonvanishing, following isobaths is the same as following f/H.

To summarize, the floats in this region spread preferentially along latitude lines or the isobaths, depending on whether they are near the boundary or not. The major difference with the North Atlantic is that there is no significant topography in the basin interior. The faster-than-linear growth in the zonal dispersion and the zero zonal mean will also be seen with interior floats in the subsequent sections.

f. South Atlantic

Next is the large set of RAFOS float trajectories from the Brazil Basin Experiment (Hogg and Owens, 1999). Some were deployed at 2500 m and others at 4000 m, so all were grouped together as "deep floats." As with the equatorial set, about half are in the interior where f/H is mostly zonal; the rest are closer to the coast of South America. For this reason the floats were subdivided into boundary and interior subsets. The trajectories were broken into 50-day pieces, as before.

As with the equatorial interior set, the f/H moments and the geographic moments for the 866 trajectories in the South Atlantic interior (Fig. 15) are very similar. There is no net drift in any direction, despite that some floats move only westward and others only eastward during the time period. The dispersion across latitude lines and f/H appears to increase linearly later on, but the zonal and along-f/H dispersions increase faster than linearly, as was also the case in the equatorial interior.

The boundary set (315 trajectories; Fig. 16) exhibit a net southward drift (of order 5 mm/s), and nearly isotropic geographic dispersion. In contrast, the mean is strongly along f/H, and the dispersion significantly anisotropic with respect to f/H. That the mean along f/H is positive is indicative of motion with shallow water to the right, which is southward along the coast of South America. The dispersion, within error, appears to increase linearly at late times, consistent with diffusion. Note too that the magnitude of the dispersion is three times greater here than in the interior, as the interior currents are generally much more sluggish.

g. North Pacific

The final set consists of 728 50-day RAFOS trajectories from the Kuroshio Extension experiment (Riser, 2000) in the North Pacific. The mean depth of these floats is 1020 m, and so they are considered subthermocline (Macdonald *et al.,* 2000). Like the equatorial and South Atlantic interiors, f/H is nearly zonal here, and most trajectories (Fig. 17) are unusually smooth and zonal. However, this is the one case where the f/H moments are clearly less anisotropic than the geographic moments.

The geographic means and dispersions indeed reflect strong zonal anisotropy, as in the other two regions. Here too the zonal dispersion is much greater than the meridional, and

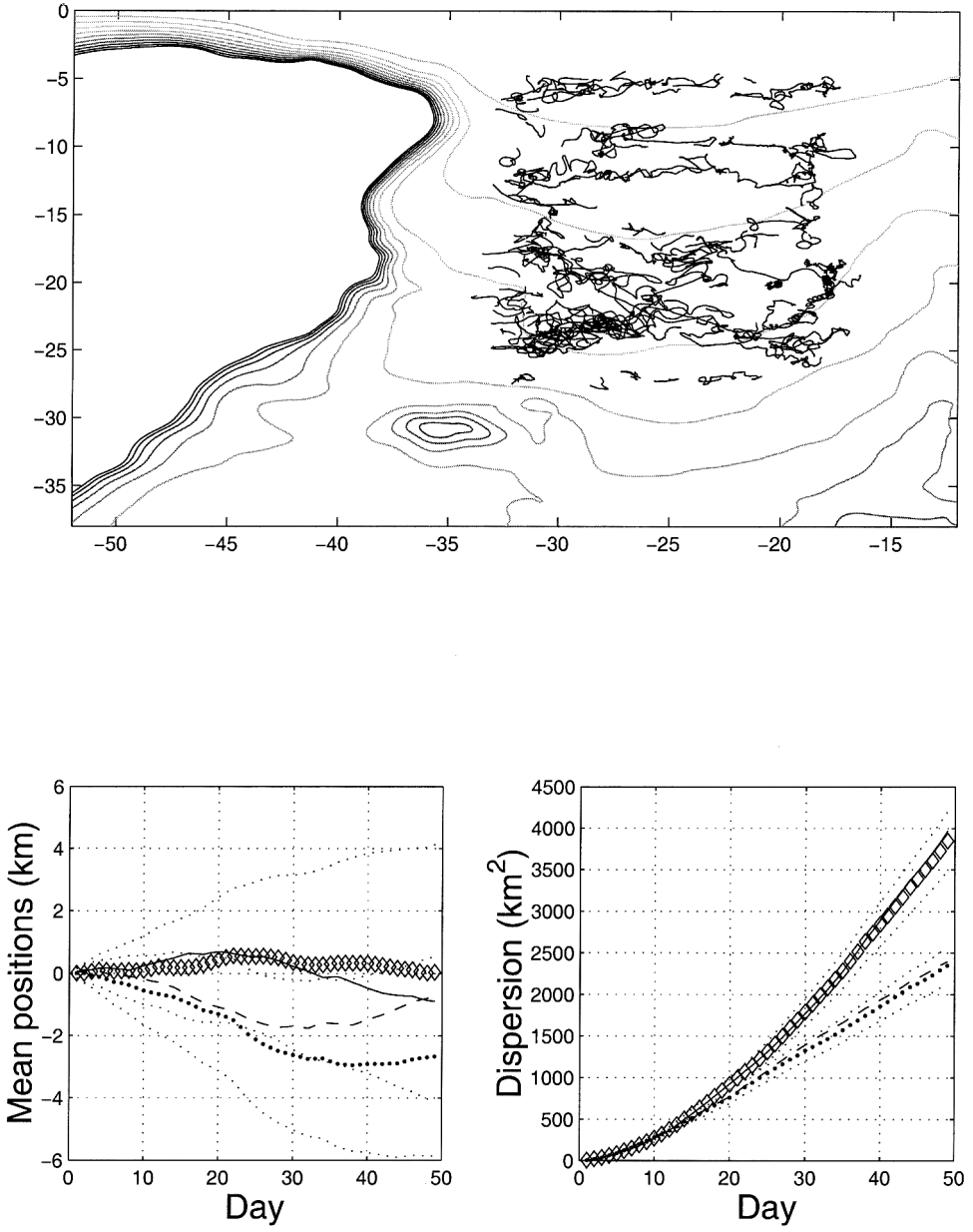

Figure 15. The results for the floats in the Brazil basin region of the South Atlantic. The contour values for f/H are $-[4\ 8\ 12 \ldots 40] * 1 \times 10^{-9}$ (ms)$^{-1}$, and the moment symbols are as in Figure 1.

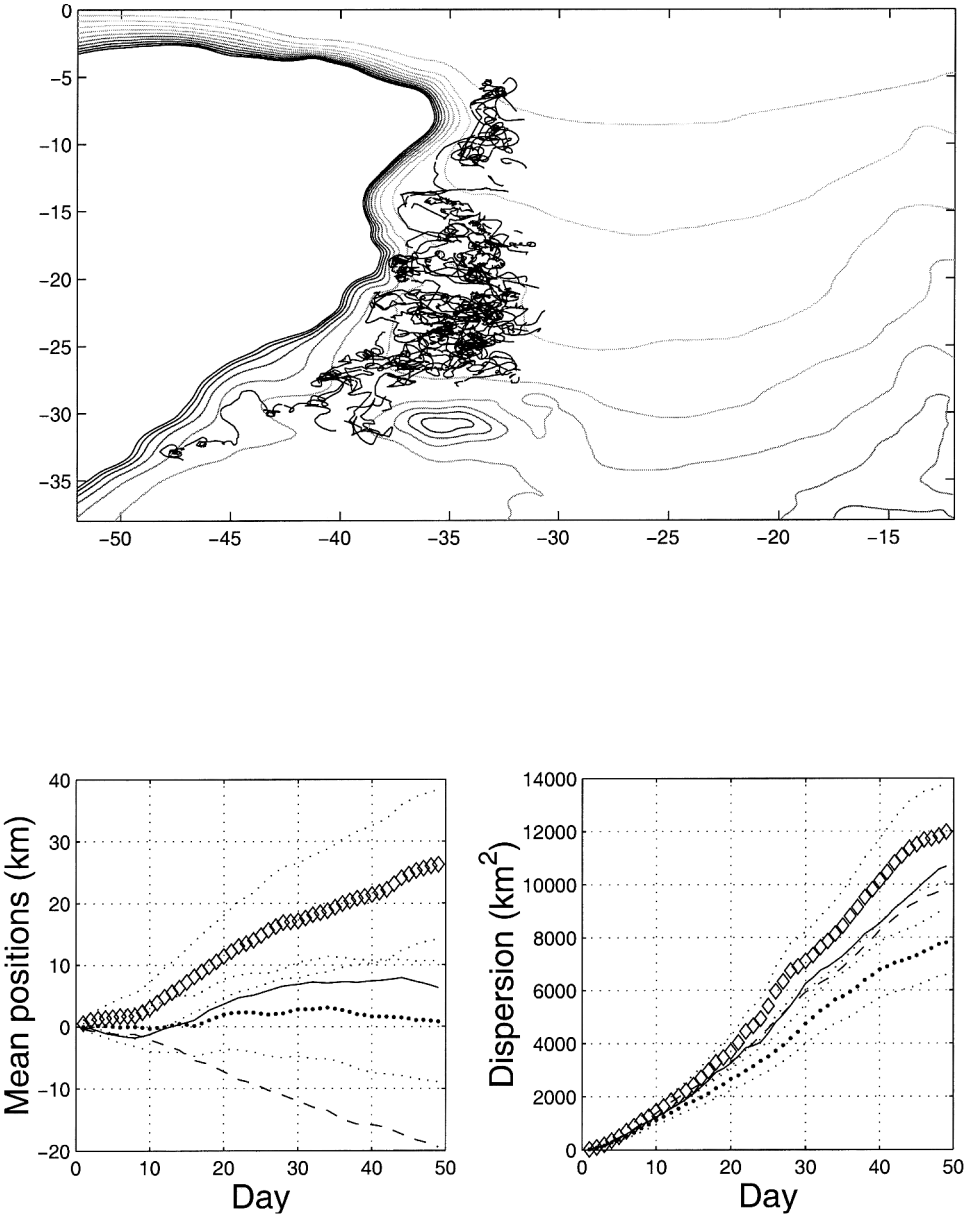

Figure 16. The results for the floats on the western boundary of the South Atlantic. The contour values are as in the preceding figure.

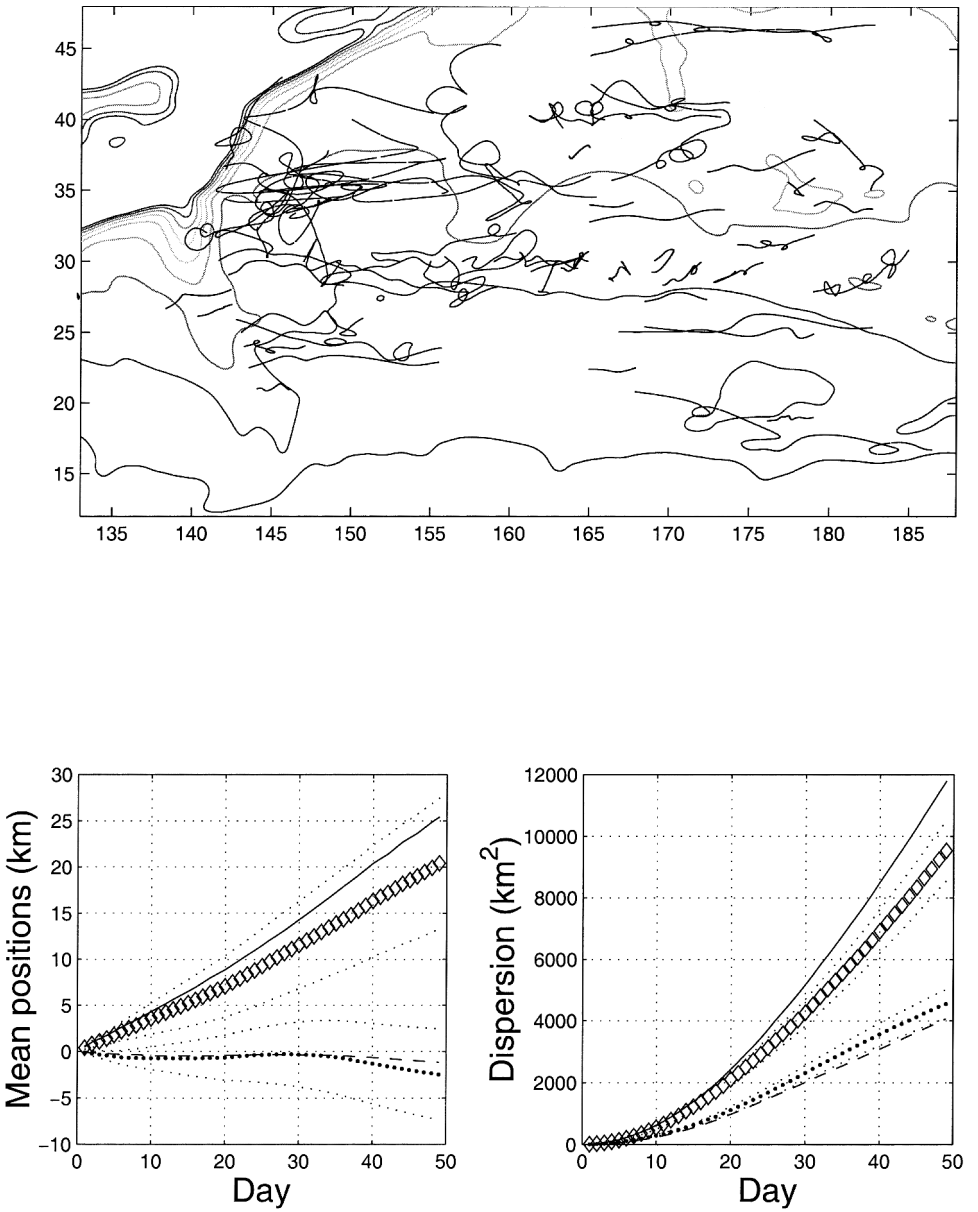

Figure 17. The trajectories and results for the floats in the North Pacific. The float depth is approximately 1000 m. The contour values for f/H are [4 8 12 . . . 40] $* 1 \times 10^{-9}$ $(\mathrm{ms})^{-1}$, and the moment symbols are as in Figure 1.

increases like $t^{3/2}$ at late times. The meridional dispersion on the other hand increases only as $t^{1/2}$, so the spreading is superdiffusive in x and subdiffusive in y. What is different here is that the mean zonal drift is significant. It is eastward, consistent with Kuroshio advection (despite the apparent lack of coherent jet-like translation events), but is also rather slow, of order 5 mm/s. The mean is not different from zero in the meridional direction.

The mean drift along f/H is greater than that across, and is not significantly different from the zonal mean. However, the dispersion along f/H is significantly less than the zonal dispersion. Indeed, while one observes floats near the Asian coast which do follow the isobaths, there are many more in the interior which move directly over topographic features.

Why the difference between the North Pacific and the Atlantic floats? At 1000 m, the floats are too deep to be directly influenced by wind forcing (Macdonald *et al.,* 2000). Rather, the answer is probably related to stratification, and to the scale of the topography. Whereas the mid-Atlantic ridge rises several thousand meters from the bottom and is as long as the Atlantic basin is wide, the Emperor Seamount chain and the Shatsky rise are much smaller than the Pacific basin and lie several thousand meters below the floats. Consistent with the notion of stratification shielding the bottom, the moments with respect to f/H are more anisotropic assuming a larger value of α, which is equivalent to increasing N/f (Fig. 10).

5. Summary and discussion

The displacements of subsurface floats in the Atlantic and Pacific oceans have been examined in relation to barotropic f/H. In all regions save the North Pacific, the displacement statistics are equally or more anisotropic relative to f/H than to f alone. In regions where the bottom is relatively flat (interior Equatorial Atlantic, interior South Atlantic, North Pacific, and portions of the interior North Atlantic) float dispersion is zonally anisotropic, and the moments relative to f/H are essentially identical to the geographical moments. Where the topography is more severe (near the western boundaries, and in the northern portion of the North Atlantic), dispersion is still anisotropic with respect to f/H, despite appearing isotropic in (x, y) or even meridionally enhanced.

One exception is in the North Pacific, where floats pass freely over deep topography. The probable explanation is that the smaller scale topography there is shielded by stratification. The other exception is near the Equatorial boundary, where floats cross f/H as they cross the equator.

The latter point in particular reminds us that the present results should not be taken as an indication of the conservation of barotropic PV. Strictly speaking, they simply indicate a statistical tendency for steering parallel to topography when the latter is severe, or zonally in flat regions. That such steering occurs may only imply that barotropic currents exist which are important to tracer transport.

It most cases, the increase in anisotropy with respect to f/H is fairly modest. But similarly modest increases can be found even in unforced barotropic model runs, if there

are no closed contours of *f/H* (LS). Greater differences are found when particles circumnavigate closed contours many times, but there are no examples of this in the present data set. Secondly, because baroclinic currents (possibly less sensitive to topography) also advect floats, the dispersion by a combination of vertical modes will likely be less aligned with *f/H* than if there were only barotropic currents.

There are several possible examples of barotropic currents which could produce spreading along *f/H*. One is planetary waves, which have an associated Lagrangian drift (Flierl, 1981; LS). As discussed in LS, waves can yield superdiffusive spreading along *f/H* with zero mean flow, similar to the observations in the equatorial and South Atlantic interiors. Flierl (1981) shows that a planetary wave's ability to transport material depends on the ratio of its advective and phase speeds. What values this ratio typically takes is not known, but Price and Rossby (1982) describe a planetary-topographic wave in the western North Atlantic with an advective speed of 12 cm/sec and a phase speed of 6 cm/sec, i.e. with a ratio of two. Such a wave could be an extremely potent transport mechanism, able to trap a substantial volume of fluid and move it *at the wave phase speed* along *f/H*.

Another possibility is that baroclinically unstable currents, like the Gulf Stream, generate barotropic variability which in turn is sensitive to topography. This might well explain the results from the western Atlantic. However, there are other conceivable explanations as well.

An intriguing finding is that the mean drift (when significant) in all deeper regions is pseudo-westward relative to *f/H* (allowing for the sign change in the southern hemisphere). This is consistent with the type of mean flow predicted by canonical equilibrium theory (Holloway, 1978; Carnevale and Frederiksen, 1987), sometimes called the "Neptune Effect" (Holloway, 1992). In the North, Equatorial and South Atlantic, the southward drift along the western boundary is attributable to the Deep Western Boundary Current, and so is arguably driven by thermohaline processes. But both the EUROFLOAT and Eastern Basin floats in the deep eastern Atlantic also display the tendency, despite being well away from western boundaries.

No consistent tendencies were found with the higher order moments (e.g. the skewness), but it is worth noting that projecting the displacements onto *f/H* induced no systematic changes in either skewness of kurtosis. Had the kurtosis changed, for example, one might worry that the present results were affected adversely by outliers. Incidentally, the kurtosis of the displacements is actually somewhat greater than the Gaussian value of three (which probably stems from the fact that Lagrangian velocities in the subsurface ocean are also non-Gaussian, as in Bracco *et al.,* 2000). This implies that the error estimates in definitions (2) and (3) could be improved.

Similar calculations were also performed with a large set of ALACE float trajectories in the Pacific (Davis, 1998). The results are not presented here, because ALACE's rise to the surface roughly every 25 days, or right in the middle of the 50-day period chosen for the analysis. But many of the floats were in relatively flat regions, and the dispersion was strongly zonal (and along *f/H*) as in similar regions discussed above. Interestingly, the

ALACE floats in the North Pacific exhibit the same tendency to cross f/H as do those floats in Section 4g, confirming that result.

To the extent that the large scale, *in situ* PV is also passive, f/H may play a role in its distribution as well. As noted, O'Dwyer *et al.* (2000) compared float trajectories to the *in situ* PV in the North Atlantic. The authors used a different method of analysis (comparing the angle made between individual float displacements and the local average inclination of the f/H contours), but found a statistical tendency for floats to move parallel to the isolines of PV. Since floats *also* follow (barotropic) f/H, it is natural to suspect the two PV fields are similar. Other authors have also speculated on topography shaping property distributions. Joyce (1981) for example noted that the mid-Atlantic ridge appears to confine the Mediterranean outflow; the latter dominates the mid-depth PV in the subtropical North Atlantic.

Using float temperature records to deduce the background stratification, Bower and Hunt (2000) showed that floats passing under the Gulf Stream tend to follow $f/H_2(t)$, where $H_2(t)$ is the depth below the thermocline. Using H_2 is clearly more sensible than H for individual (deep) floats, with regards to the conservation of PV. That the barotropic f/H appears to work here is probably due to averaging many individual trajectories, so that the deviations from thermocline motion are smoothed out.

The present focus was on displacements, but there are other possible measures one could use. For instance, there are the moments of the values of f/H that the floats "see" at each instant (LS). Such a measure accounts naturally for variable f/H gradients, unlike the projected displacements. However, it must be "calibrated" in some way, for instance by comparing with stochastic float trajectories. This calculation was in fact done for all the aforementioned sets, and the means and dispersions for the actual floats were always less than or equal to those for the stochastic floats, which again is consistent with a reluctance to cross contours by the floats. Other measures are possible, and perhaps preferable to those presented here.

More data would be very helpful in terms of sorting out differences between different ocean basins. In particular, data from the deep Pacific and from the Indian Ocean will obviously be of great interest.

6. Conclusions

The present results suggest that Lagrangian dispersion in the ocean is sensitive to barotropic f/H, despite the presence of stratification and forcing. This is not to say that the ocean behaves as an unforced, barotropic fluid, rather that currents exist in most regions which favor such steering. As such, it may be advantageous to discuss particle dispersion with respect to this field (or another more optimal field) rather than simply in the zonal and meridional directions. The same comment applies to the parameterization of transport of quantities like heat and salt.

Acknowledgments. The work was supported under MAST PL920057 (while I was visiting IFREMER in Brest, France) and in part by the Charles Davis Hollister Fund and the Penzance Endowed Fund for assistant scientist support at W.H.O.I. I had many enjoyable conversations with Kevin Speer, and many helpful comments from Russ Davis, Lien Hua, Steve Lentz, Breck Owens, Volfango Rupolo and from some anonymous reviewers. Thanks to Breck Owens and Nelson Hogg for the Deep Basin Experiment data, to Kevin Speer for the EUROFLOAT data, to Tom Rossby for an early look at his North Atlantic Current data and to Russ Davis for the ALACE data in the Pacific. This is W.H.O.I. contribution number 9945.

REFERENCES

Anderson-Fontana, S. and H. T. Rossby. 1991. RAFOS floats in the SYNOP Experiment: 1988–1990. University of Rhode Island, G. S. O. Tech. Rept. 91–7. 155 pp.

Batchelor, G. K. and A. A. Townsend. 1953. Turbulent Diffusion. Surveys in Mechanics, *23,* 352–398.

Bower, A. and H. Hunt. 2000. Lagrangian observations of the Deep Western Boundary Current in the North Atlantic ocean; part II, the Gulf Stream-Deep Western Boundary Current crossover. J. Phys. Oceanogr., *30,* (in press).

Bracco, A., J. H. LaCasce and A. Provenzale. 2000. Velocity pdfs for oceanic floats. J. Phys. Oceanogr., *30,* 461–474.

Bretherton, F. B. and D. Haidvogel. 1976. Two-dimensional turbulence over topography. J. Fluid Mech., *78,* 129–154.

Carnevale, G. F. and J. S. Frederiksen. 1987. Nonlinear stability and statistical mechanics of flow over topography. J. Fluid Mech., *175,* 157–181.

Cheney, R. E., W. H. Gemmill, M. K. Shank, P. L. Richardson and D. Webb. 1976. Tracking a Gulf Stream ring with SOFAR floats. J. Phys. Oceanogr., *6,* 741–749.

Davis, R. E. 1991. Observing the general circulation with floats. Deep-Sea Res., *38* (Suppl.), S531–S571.

—— 1998. Preliminary results from directly measuring mid-depth circulation in the Tropical and South Pacific. J. Geophys. Res., *103,* 24619–24639.

Flierl, G. R. 1981. Particle motions in large-amplitude wave fields. Geophys. Astrophys. Fluid Dyn., *18,* 39–74.

Freeland, H. J., P. B. Rhines and T. Rossby. 1975. Statistical observations of the trajectories of neutrally buoyant floats in the North Atlantic. J. Mar. Res., *33,* 383–404.

Griffa, A., K. Owens, L. Piterbarg and B. Rozovskii. 1995. Estimates of turbulence parameters from Lagrangian data using a stochastic particle model. J. Mar. Res., *53,* 371–401.

Hogg, N. G. and W. B. Owens. 1999. Direct measurements of the deep circulation within the Brazil Basin. Deep-Sea Res., *46,* 335–353.

Holloway, G. 1978. A spectral theory of nonlinear barotropic motion above irregular topography. J. Phys. Oceanogr., *8,* 414–427.

—— 1992. Representing topographic stress for large-scale ocean models. J. Phys. Oceanogr., *22,* 1033–1046.

Joyce, T. M. 1981. The influence of the mid-Atlantic ridge upon the circulation and the properties of the Mediterranean Water southwest of the Azores. J. Mar. Res., *39,* 31–52.

Joyce, T. M., J. R. Luyten, A. Kubryakov, F. B. Bahr and J. S. Pallant. 1998. Meso to large-scale structure of subducting water in the subtropical gyre of the eastern North Atlantic. J. Phys. Oceanogr., *28,* 40–61.

LaCasce, J. H. and K. Speer. 1999. Lagrangian statistics in unforced barotropic flows. J. Mar. Res., *57,* 245–275.

Leaman, K. D. and P. Vertes. 1994. Pathways in the Deep Western Boundary Current recirculation south of 30N. University of Miami, RSMAS Tech. Rept. 94-002, 100 pp.

Li, Xianjin, P. Chang and R. C. Pacanowski. 1996. A wave-induced stirring mechanism in the mid-depth equatorial ocean. J. Mar. Res., *54,* 487–520.

Macdonald, A. M., T. Suga and R. G. Curry. 2000. An isopycnally averaged North Pacific climatology. J. Geophys. Res., (submitted).

Marshall, D. 1995. Influence of topography on the large-scale ocean circulation. J. Phys. Oceanogr., *25,* 1622–1635.

McWilliams, J. C. 1976. Maps from the Mid-Ocean Dynamics Experiment: Part II. Potential vorticity conservation. J. Phys. Oceanogr., *6,* 828–846.

O'Dwyer, J., R. G. Williams, J. H. LaCasce and K. G. Speer. 2000. Does the PV Distribution constrain the spreading of Floats in the N. Atlantic? J. Phys. Oceanogr. *30,* (in press).

Ollitrault, M. 1995. La circulation générale de l'Atlantique Nord subtropical vers 700 m de profondeur, révélée par des flotteurs dérivants de subsurface. C. R. Acad. Sci. Paris, *321,* 153–160.

Ollitrault, M., P. Tillier, I. Bodevin and H. Klein. 1988. Deep SOFAR float experiment in the North-East Atlantic. Institut Francais de Recherche pour l'Exploitation de la Mer Tech. Rept., *11,* 122 pp.

Owens, W. B. 1984. A synoptic and statistical description of the Gulf Stream and subtropical gyre using SOFAR floats. J. Phys. Oceanogr., *14,* 104–113.

—— 1991. A statistical description of the mean circulation and eddy variability in the northwestern Atlantic using SOFAR floats. Prog. Oceanogr., *28,* 257–303.

Owens, W. B. and N. G. Hogg. 1980. Oceanic observations of stratified Taylor columns near a bump. Deep-Sea Res., *27A,* 1029–1045.

Pedlosky, J. 1987. Geophysical Fluid Dynamics, Springer-Verlag, 710 pp.

Price, J. F., T. M. McKee, W. B. Owens and J. R. Valdes. 1987. Site L SOFAR float experiment, 1982–1985. Woods Hole Oceanographic Institution Technical Report, WHOI-, WHOI-97-52. 289 pp.

Price, J. F. and H. T. Rossby. 1982. Observations of a barotropic planetary wave in the western North Atlantic. J. Mar. Res., *40* (Suppl.), 543–557.

Rees, J. M. and E. M. Gmitrowicz. 1989. Dispersion measurements from SOFAR floats on the Iberian abyssal plain, *in* Interim Oceanographic Description of the North-East Atlantic Site for the Disposal of Low-Level Radioactive Waste, Vol. 3, F. Nyffeler and W. Simmons, eds., Nuclear Energy Agency, OECD, Paris, 64–67.

Rhines, P. B. 1970. Edge-, bottom- and Rossby waves in a rotating, stratified fluid. Geophys. Fluid Dyn., *1,* 273–302.

Richardson, P. L. 1982. Gulf Stream paths measured with free-drifting buoys. J. Phys. Oceanogr., *11,* 999–1010.

Richardson, P. L., Hufford, G. E. and R. Limeburner. 1994. North Brazil Current retroflection eddies. J. Geophys. Res., *99,* 5081–5093.

Richardson, P. L. and W. J. Schmitz, Jr. 1993. Deep cross-equatorial flow in the Atlantic measured with SOFAR floats. J. Geophys. Res., *98,* 8371–8387.

Richardson, P. L., D. Walsh, L. Armi, M. Schroder and J. F. Price. 1989. Tracking three Meddies with SOFAR floats. J. Phys. Oceanogr., *19,* 371–383.

Riser, S. C. 1982. The quasi-Lagrangian nature of SOFAR floats. Deep-Sea Res., *29,* 1587–1602.

—— 2000. Lagrangian measurements of the subsurface flow in the Northwest Pacific. J. Phys. Oceanogr. (submitted).

Riser, S. C. and H. T. Rossby. 1983. Quasi-Lagrangian structure and variability of the subtropical western North Atlantic circulation. J. Mar. Res., *41,* 127–162.

Rossby, H. T. 1996. The North Atlantic Current and surrounding waters: At the crossroads. Rev Geophys., *34,* 463–481.

Rossby, H. T., A. S. Bower and P. T. Shaw. 1985. Particle pathways in the Gulf Stream. Bull. Amer. Meteor. Soc., *66,* 1106–1110.

Rossby, H. T., J. F. Price and D. Webb. 1986. The spatial and temporal evolution of a cluster of SOFAR floats in the POLYMODE Local Dynamics Experiment (LDE). J. Phys. Oceanogr., *16,* 428–442.

Rossby, H. T., S. C. Riser and A. J. Mariano. 1983. The western North Atlantic—a Lagrangian viewpoint, *in* Eddies in Marine Science, A. R. Robinson, ed., Springer-Verlag, Berlin. 609 pp.

Rossby, H. T., A. D. Voorhis and D. Webb. 1975. A quasi-Lagrangian study of mid-ocean variability using long-range SOFAR floats. J. Mar. Res., *33,* 355–382.

Rupolo, V., B. L. Hua, A. Provenzale and V. Artale. 1996. Lagrangian velocity spectra at 700 m in the Western North Atlantic. J. Phys. Oceanogr., *26,* 1591–1607.

Sawford, B. L. 1993. Recent developments in the Lagrangian stochastic theory of turbulent dispersion. Boundary Layer Meteor., *62,* 197–215.

Schmitz, W. J., Jr. 1985. SOFAR float trajectories associate with the Newfoundland Basin. J. Mar. Res., *43,* 761–778.

Schmitz, W. J. Jr., W. R. Holland and J. F. Price. 1983. Mid-latitude mesoscale variability. Rev. Geophys. Space Phys., *21,* 1109–1119.

Schmitz, W. J., Jr., J. F. Price, P. L. Richardson, W. B. Owens, D. C. Webb, R. E. Cheney and H. T. Rossby. 1981. A preliminary exploration of the Gulf Stream system with SOFAR floats. J. Phys. Oceanogr., *11,* 1194–1204.

Solomon, T. H., E. R. Weeks and H. L. Swinney. 1993. Observation of anomalous diffusion and Levy flights in a two-dimensional rotating flow. Phys. Rev. Lett., *71,* 3975–3978.

Spall, M. A., P. L. Richardson and J. F. Price. 1993. Advection and eddy mixing in the Mediterranean salt tongue. J. Mar. Res., *51,* 797–818.

Speer, K. S., J. W. Gould and J. H. LaCasce. 1999. Year-long trajectories of floats in Labrador Sea Water in the eastern North Atlantic Ocean. Deep-Sea Res. II, *46,* 165–179.

Sundermeyer, M. A. and J. F. Price. 1998. Lateral mixing and the North Atlantic Tracer Release Experiment: Observations and numerical simulations of Lagrangian particles and passive tracer. J. Geophys. Res., *103,* 21481–21497.

Taylor, G. I. 1921. Diffusion by continuous movements. Proc. Lond. Math. Soc., *20,* 196–212.

—— 1953. Dispersion of soluble matter in solvent flowing slowly through a tube. Proc. Roy. Soc. Lond. Ser. A, *219,* 186–203.

Wunsch, C. 1981. Low-frequency variability of the sea, *in* Evolution of Physical Oceanography, B. A. Warren and C. Wunsch, eds. The MIT Press, 342–375.

Zenk, W., K. S. Tokos and O. Boebel. 1992. New observations of meddy movement south of the Tejo plateau. Geophys. Res. Lett., *19,* 2389–2392.

Zhang, H-M, M. D. Prater and T. Rossby. 2000. Isopycnal Lagrangian statistics from the North Atlantic RAFOS float observations. J. Geophys. Res., (submitted).

Received: *27 July, 1999;* revised: *3 January, 2000.*